

ELECTRICAL PROPERTIES OF OXIDE GLASSES WITH ALUMINIUM DISPERSOIDS

by

ABHA RANI SINGH



MATERIALS SCIENCE PROGRAM
INDIAN INSTITUTE OF TECHNOLOGY, KANPUR
July 1986

MSP
1986
M
SIN
ELE

ELECTRICAL PROPERTIES OF OXIDE GLASSES WITH ALUMINIUM DISPERSOIDS

A Thesis Submitted
in Partial Fulfilment of the Requirements
for the Degree of
MASTER OF TECHNOLOGY

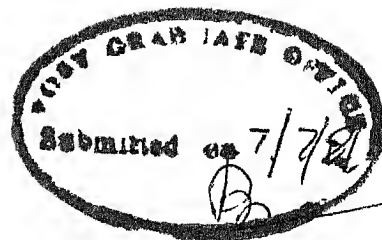
by
ABHA RANI SINGH

to the
MATERIALS SCIENCE PROGRAM
INDIAN INSTITUTE OF TECHNOLOGY KANPUR
July 1986

23 SEP 1987
CENTRAL LIBRARY

Acc No **A** 98043

MSP-1906-M-SIN-ELE



CERTIFICATE

This is to certify that the thesis entitled "Electrical Properties of Oxide Glasses with Aluminium Dispersoids" by Miss Abha Rani Singh is carried out under my supervision and has not been submitted elsewhere for a degree

D Chakravorty
D Chakravorty
Professor
Materials Science Programme
Indian Institute of Technology
Kanpur - 208016

ACKNOWLEDGEMENT

With the culmination of the proposed work and compilation in this form of dissertation, I have an opportunity to accord my sincere thanks to Dr D Chakravorty for his astute guidance and keen interest in this work. He provided me necessary manoeuvrability and freedom to work, albeit keeping a watchful eye on the progress.

I sincerely acknowledge the help rendered to me by the staff of the Advanced Centre for Materials Science.

I would like to record my sincere appreciation to Mr B Sharma for his unflinching co-operation during the experimental work.

I do record my deep sense of gratitude to Mr B.K Jain and Mr V P. Gupta for making excellent drawings.

A special word of appreciation to Mr S R Bhardwaj for his excellent typing.

Last but not the least, the co-operation and help of my friends is thankfully acknowledged.

CONTENTS

Page

LIST OF TABLES

LIST OF FIGURES

ABSTRACT

CHAPTER

1	- INTRODUCTION	2
1 1	- MICROSTRUCTURAL STUDIES	
1 2	- Electrical Properties of Glass Metal Microcomposites	5
1 2 1	- Switching Studies	5
1 2 2	- Electrical Conductivity	7
1 2 3	- Temperature Dependence of Electrical conductivity	7
1 2 4	- Variation of A C Conductivity with frequency	9
1 3	- Ion Exchange and Reduction	10
1 4	- Objective of present investigation	12
2	- EXPERIMENTAL TECHNIQUES	13
2 1	- Preparation of glass	13
2 2	- Sample Preparation for Electrical Resistivity Measurement.	13
2 3	- Conductivity cell	14
2 4	- Resistivity Measurement Complex Impedance Analysis of A C Data	15
2 5	- X-ray Analysis	16

	Page
2 6 - Electron Microscopic Analysis by TEM	17
2 6 1 - Sample Preparation	17
2 7 - Density Measurement	19
2 8 - Differential Scanning Calorimetry	19
2 9 - Ion Exchange	20
2 10 - Sample Preparation for Ion-exchange	21
3 - RESULTS AND DISCUSSION	22
3 1 - Transmission Electron Microscopic Analysis	22
3 1 1 - MICROSTRUCTURE	22
3 1 2 - Selected Area Diffraction	22
3 2 - Differential Scanning Calorimetry	23
3 3 - X-ray Analysis	23
3 4 - Density of the Glasses	23
3 5 - A C Measurement and Complex Impedance Analysis	23
3 6 - Temperature Dependence of Resistivity	24
3 7 - ϵ' Vs log f plot	26
TABLES	28-33
FIGURES	34-67
REFERENCES	68-70

LIST OF TABLES

<u>S.No.</u>	<u>Table No.</u>		<u>Page</u>
1	2 1 1	- Composition and density of the different glass samples	28
2	3 1.2	- SAD of the Gold film for the calculation of camera constant	29
3	3 2 3	- SAD of the glass sample A2: calculation of d_{hkl} values	29
4	3 3 4	- Comparison of d_{hkl} values of Aluminium with those obtained from SAD of glass sample A2 (Glass containing 10 mole% of Al)	30
5	3 4 5	- Glass Transition Temperature (T_g) for the glass system	31
	3 5 6	- Activation energy (Q) and pre-exponential factor (ρ_0) for the glass system	32
	3 6.7	- Activation energy (Q) and Pre-exponential factor for the ion-exchanged glasses	33

LIST OF FIGURES

	Page
2 1 1 - Schematic view of the conductivity cell	34
2 2 2 - Schematic circuit diagram for AC resistivity measurement	35
3 1 3 - Electron micrograph of glass sample A2 x 181730	36
3 2 4 - Electron diffraction pattern for gold film	37
3 3 5 - Electron diffraction pattern of the glass sample A2	38
3.4 6 - Differential scanning calorimetry for different glass samples	39
3 5 7 - X-ray analysis for sample A1	40
3 6 8 - X-ray analysis for sample A2	41
3 7 9 - X-ray analysis for sample A3	42
3 8 10 - X-ray analysis for sample A4	43
3 9 11 - Complex impedance plot for glass sample A1 ($T = 125^{\circ}\text{C}$)	44
3 10 12- Complex impedance plot for glass sample A2 ($T = 100^{\circ}\text{C}$)	45
3 11 13- Complex impedance plot for glass sample A3 ($T = 103^{\circ}\text{C}$)	46
3 12 14- Complex impedance plot for glass sample A4 ($T = 175^{\circ}\text{C}$)	47
3 13 15- Complex impedance plot for glass sample I A1 ($T = 303^{\circ}\text{C}$)	48
3 14 16- Complex impedance plot for glass sample I A2 ($T = 191^{\circ}\text{C}$)	49
3 15 17- Complex impedance plot for glass sample I A3 ($T = 80^{\circ}\text{C}$)	50

	Page
3 16 18 - Complex impedance plot for glass sample I A4 ($T = 230^{\circ}\text{C}$)	51
3 17 19 - Log ρ Versus $1/T$ plot for glass sample A1	52
3 18 20 - Log ρ Versus $1/T$ plot for glass sample A2	53
3 19 21 - Log ρ Versus $1/T$ plot for glass sample A3	54
3 20 22 - Log ρ versus $1/T$ plot for glass sample A4	55
3 21 23 - Log ρ versus $1/T$ plot for glass sample I A1	56
3 22 24 - Log ρ versus $1/T$ plot for glass sample I A2	57
3 23 25 - Log ρ versus $1/T$ plot for glass sample I A3	58
3 24 26 - Log ρ versus $1/T$ plot for glass sample I A4	59
3 25 27 - Log ρ versus $1/T$ plot for glasses A1, A2, A3, A4	60
3 26 28 - Log ρ versus $1/T$ plot for glass samples A1 and I A1	61
3.27 29 - Log ρ versus $1/T$ plots for glass samples A2 and I A2	62
3 28 30 - Log ρ versus $1/T$ plots for glass samples A4 and I A4	63
3.29 31 - ϵ' versus log f plot for glass sample A1	64
3 30 32 - ϵ' versus log f plot for glass sample A2	65

3 31 33 -	ϵ' versus log f plot for glass sample A3 (T = 103°C)	66
3 32 34 -	ϵ' versus log f plot for glass sample A4	67

ABSTRACT

Presence of ultrafine metallic granules in alkali containing glass has a significant effect on its electrical conductivity. The glass metal microcomposites with aluminium as a dispersion metal in the glass matrix have been prepared. Role of metallic dispersoids on ionic conductivity of alkali containing glasses and that of their ion exchanged versions has been investigated. It is found that there is enhancement in electrical conductivity of glasses by metallic dispersion and ion-exchange treatment. It has been further observed that highly conducting glasses with very low values of activation energy can be developed.

Chapter I (Introduction) deals with the various applications of the glass-metal microcomposites and the literature survey.

Chapter 2 describes the Experimental techniques used to prepare and characterise the glass-samples with different mole% of aluminium. Procedure for ion-exchange treatment of these glasses has been described. The characterization techniques include A.C. electrical resistivity measurements, Transmission electron microscopy, density measurement, X-ray analysis and Differential Scanning Calorimetry to get the glass transition temperature of different glass samples.

In Chapter 3, results and A.C. conductivity of glass-metal composites containing aluminium metal dispersoids

have been reported. Mole percent of aluminium has been varied from 0 to 20. Presence of aluminium particles enhances the electrical conductivity of virgin and ion-exchanged samples.

Chapter - 1

INTRODUCTION

Glass-metal microcomposites as the name suggests are glasses, in which, metal particles of dimension of the order of few hundred angstroms are precipitated in the matrix. Metal colloids¹ of gold, silver and copper are well known for their application to produce colored glasses, particularly red colour which can not be induced by ionic colouring methods. These glasses have attracted the attention of glass scientists/technologists during the last few decades because of their wide practical applications. The applications of glass-metal microcomposites may broadly be classified as follows: Photo sensitive glasses^{2,3}, photosensitively nucleated glasses ceramics⁴, photochromic glasses⁵, polychromatic glasses⁶, photothermal conversion (cermet)⁷, solar control coatings (electrofloat process⁸). Apart from these, the other possible applications are: Electroconducting glasses and fibres⁹, memory and threshold switching^{10,11}, high strength glasses and Fibres¹². These applications require a suitable method of metal precipitation in glass matrix. These methods can be summarised as follows:

1. Reduction during melting and controlled cooling of the melt¹³
2. Exposure of the glass to high energy X-ray, γ -ray or UV radiation and subsequent heat treatment¹⁴.

- 3 Staining process in which metal salt is pasted on the glass surface and baked at higher temperature¹⁵
- 4 Ion-exchange and reduction treatments¹⁶

Many of the glasses prepared in these manner exhibit interesting optical properties and therefore lead to their wide applications in window glasses, lenses, containers, lasers, filters, waveguides etc

Glass containing bismuth and selenium particles have received attention in recent years because of their interesting electrical properties specially the switching effect^{10,11,17}, after these glasses were subjected to sodium \rightleftharpoons silver ion-exchange followed by a reduction treatment in hydrogen. This behaviour has been attributed to microstructural characteristic of glass which reveals the presence of bismuth islands in the matrix

1.1 MICROSTRUCTURAL STUDIES

The metallic granules in the glass-metal microcomposites can be resolved by transmission electron-microscope. There are various methods available for precipitation of metallic particles.

^{18,19} Doremus prepared photosensitive glasses containing gold and silver by the introduction of metal in its chloride form and CeO_2 as nucleating agent. The glasses were irradiated by UV radiation to develop nucleation sites and heat-treatment was given to get metal particles of 9-11 nm in size.

Glass metal microcomposites containing silver and bismuth particles of size 5-200 nm dispersed in glass matrix were prepared by subjecting glass surface to ion exchange reaction followed by reduction treatment in hydrogen atmosphere²⁰. Such glasses show memory switching and high conductivity values

The droplet phase in virgin specimen of Sb_2O_3 containing glass is found to be rich in antimony but not in metallic state. The ion exchanged and reduced specimen has a structure consisting of fine silver droplets of diameters measuring from 50 - 100 Å.

In case of Al_2O_3 containing glasses the droplet phase in virgin sample is rich in bismuth which however is not in metallic state. After ion exchange and reduction the droplets become much smaller ranging from 50 - 150 Å and after reduction metallic silver droplets appear having diameters measuring from 50 - 650 Å.

It is to be noted that in all the cases metallic silver particles with diameters measuring from 50 - 2000 Å are found to appear in dispersed glass matrix.

Phosphate and silicate glasses containing metallic bismuth²¹ in the matrix were prepared by reducing the metal oxide in hydrogen atmosphere. In this process bismuth particles of dimension 5-20 nm emerged in the glass matrix. These glasses also showed memory and threshold switching. The studies pertaining to glasses belonging to $\text{Na}_2\text{O} - \text{B}_2\text{O}_3$ and $\text{PbO} - \text{B}_2\text{O}_3$ systems containing Bi_2O_3 reveal in the micro-structure the presence of metallic bismuth granules with its oxide dispersed in glassy matrix. At low temperatures, the conductivity was found to be electronic while at high temperatures, it was ionic²².

Sodium aluminosilicate glasses containing small gold

and silver particles were studied by Doremus and Furkalo²³
 These particles were grown in size by irradiating the glass
 by UV radiation and subsequent heat treatment. The particles
 grown in this manner showed a uniform size in a particular
 sample.

Pilkingtons⁵ developed electrofloat process to produce
 coatings on window glasses. This is based on field induced ion-
 exchange followed by reduction, one of the ion exchange species
 being copper. The microstructure of such product has micros-
 pheres of copper distributed in the glass matrix.

The electron micrograph of the surface of "Float"²⁴
 glass shows no phase separation before ion exchange and
 reduction treatment. After sodium \rightleftharpoons copper ion exchange done
 at high temperature (650°C) the sample shows phase separation
 due to injection of copper ions into glass. Similar electron
 microscopic investigation has been carried out on two oxide
 glasses containing alkali ion²⁵ subjected to sodium \rightleftharpoons silver
 ion exchange followed by reduction in hydrogen atmosphere at
 various temperatures. Silver rich phases of size 3 - 50 nm
 with metallic silver embedded in them were obtained.

Sodium silicate glasses²⁶ were heated in molten silver
 chloride bath at 600°C, which led to the diffusion of silver
 ions in the glass matrix. The microstructures of these glasses
 were used to calculate the size of silver particles which
 ranged between 1-10 nm depending on staining time. Smithhard
 and Dupree²⁷ studied the microstructure of glasses containing
 a large number of well characterized small (1-10 nm) silver

particles These particles were produced in glass matrix by staining and photosensitisation method

1 2 ELECTRICAL PROPERTIES OF GLASS METAL MICROCOMPOSITES:

1 2 1 SWITCHING STUDIES

Oxide glasses containing metallic granules of dimensions of the order of a few hundred angstroms show electrical conduction by an electron tunneling mechanism between the metallic island¹⁷ such glasses show high conductivity Surface layers of certain borosilicate glasses containing bismuth and selenium granules show memory switching after these were subjected to a sodium silver ion exchange following by a reduction treatment in hydrogen¹¹ Measurements carried out on thick films of these glasses which have not been subjected to any ion exchange and to reduction treatments show that the switching action is the characteristic feature of the base glass itself, the role of silver particles being only to lower the switching voltage²² The off state resistance of these glass films has been tentatively explained as arising due to electron hopping between the metallic islands of bismuth

Memory switching has been observed by Chakravorty et al²⁰ in surface layers containing Bi_2O_3 and Sb_2O_3 separately in $\text{Na}_2\text{O} - \text{B}_2\text{O}_3 - \text{SiO}_2$ base glass matrix Chakravorty and Murthy²⁸ have observed negative resistance and memory

switching in thin films of $\text{Na}_2\text{O}-\text{Bi}_2\text{O}_3-\text{B}_2\text{O}_3-\text{SiO}_2$ glasses

It is to be noted that the surface roughness of the glass is necessary for obtaining the high conductance effect. It is believed that imperfections introduced in the surfaces by grinding operation increases the efficiency of metallic particles which can then grow sufficiently to form a continuous chain.

Chakravorty et al.²⁸ have shown that in case of thin films of bismuth glasses, there is a possibility for the "Off" state conduction to the electron hopping between the conducting islands of bismuth. The activation energy for electron hopping in such a situation is given by $e^2/\epsilon r$ ²⁹ where ϵ is the dielectric constant of glass matrix, and r is the diameter of the conducting island.

WH Omar et al.³⁰ have shown that the negative resistance obtained in these glass films is considered to arise from a Joule-microheating process. It has been found by the extrapolation of the plot of threshold voltage versus temperature for the glass films, that at about 450°C, the glass shows switching without the application of electric field and switches "Off" at the temperature close to the melting point of the bismuth metal. In the temperature range 500 - 600°C, these glasses tend to crystallize with the crystalline phase having a lower resistance than the parent glass.

The "ON" state is assumed to be result of the formation

of bismuth filaments between conducting islands. The switch "Off" process can be explained by the rupture of the filament

Whether the glass will show "threshold" or memory switching depends on its chemical composition. For instance, a glass with composition 10 Ge - 30 As - 12.6 Si - 47.7 Te (atomic percent) shows threshold switching whereas another one with composition 10 Ge - 50 As - 40 Te (atomic percent) shows memory behaviour³¹

1.2.2 ELECTRICAL CONDUCTIVITY:

Conduction in glasses can be either ionic or electronic in nature depending upon the nature of glass and the temperature range.

1.2.3 TEMPERATURE DEPENDENCE OF ELECTRICAL CONDUCTIVITY:

The temperature dependence of electrical conductivity can be explained by diffusion mechanism³² (Jain et al 1984) which leads to an equation:

$$\sigma = \frac{A}{T} \exp\left(\frac{-H}{kT}\right) \quad . \quad 1.1.1$$

$$\text{where } A = \frac{A' N e^2 \nu d^2 c}{T} \exp\left(\frac{-S}{K}\right)$$

with N = total concentration of the given ions per unit volume e, k, T have usual meanings.

S, H = entropy and enthalpy associated with the jump step

d = jump distance

ν = attempt frequency

C = fraction of mobile species

A' = constant related to lattice geometry

In eqn (1 1 1) A is temperature independent pre-exponential factor

A close examination of recent electrical conductivity^{33,34} data obtained using A C complex impedance analysis on alkali conducting glasses show small but definite departure from equation (1 1.1)

Moynihan et al³⁵ have analyzed their data after modifying eqn (1 1 1)

$$\sigma = AT^m \exp\left(\frac{-H}{KT}\right) \quad 1 2 \rangle$$

where m = fitting parameter

The m = 0 describes the data within experimental error (which is also predicted by Transition State theory³⁶ and therefore suggest it as a better expression for temperature dependence of conductivity of glasses Eqn (1 2 2) has been frequently used in literature with the name RASCH and HINRICHSSEN relation³⁷

Chakravorty¹⁷ considers the Arrhenious type of variation of resistivity as a function of temperature

$$\rho = \rho_0 \exp\left(\frac{B}{KT}\right) \quad 1 3 3$$

Abeles et al³⁸ have shown that for low electric fields the resistivity of granular metals when the particles are isolated from each other, is given by:

$$\rho = \rho_0 \exp 2\left(\frac{C}{KT}\right)^{1/2} \quad 144$$

where ρ_0 is a constant

$$C = \chi S E_c^0$$

$$\chi = \left(\frac{2m\phi}{h^2}\right)^{1/2}$$

$$E_c^0 = \frac{2e^2}{Kd} \quad \text{with } K = \epsilon \left(1 + \frac{d}{2S}\right)$$

m = electronic mass

ϕ = effective barrier height

h = Planck's constant

S = Separation between grains

E_c^0 = energy required to generate a pair of fully dissociated positively and negatively charged grains.

ϵ = dielectric constant of an insulating medium

d = grain size

The dc resistivity data for bismuth and selenium containing glasses have been plotted as $\log \rho$ against $\frac{1}{T^{1/2}}$ which shows a linear curve and confirming the tunneling mechanism between the conducting islands (Chakravorty et al ¹⁷).

1 2 4 VARIATION OF AC CONDUCTIVITY WITH FREQUENCY:

Chakravorty et al ¹⁷ has plotted the variation of A C resistivity as a function of frequency. The A C conductivity obeys a relation of the type $\sigma(f) \propto f^n$ with n having a value around 0.9 in the region of 10^6 Hz. This is attributed to a Maxwell - Garnet mechanism in an inhomogeneous conductor (Abeles et al).

1 3 ION EXCHANGE AND REDUCTION:

It is found that the resistivity of certain oxide glasses will decrease if the surface is given reduction treatment by hydrogen. Green and Blodgett³⁹ have studied the electrical properties of Bi_2O_3 and PbO glasses after subjecting to reduction treatment by hydrogen. They have found that the surface conductivity of the reduced glasses is very low ($\approx 100 - 1000$ ohm/square) and it depends on the distance between the particles, influence of surrounding oxide lattices and composition of the glasses⁴⁰

When a glass is ion-exchanged by Ag^+ , Cu^+ or Cu^{++} ions is carried out about the glass transition Temperature T_g , the network of glass adjusts itself to the differing partial molar volumes of the exchange ions when the temperature is less than T_g , it results in stress in the glass. If the salt bath ions are larger than the host ions in the glass, there is a resultant compression which increases the strength of the glass⁴¹.

S. Sakka et al.⁴² worked on the incorporation of copper into aluminosilicate glass by Cu-Na ion-exchange at 550°C . The results can be summarized as follows

The Cu-Na ion exchange rate examined with the glass $20 \text{ Na}_2\text{O}$, 10 CaO , 70 SiO_2 (mole %) increased with increasing temperature in the range of $500 - 650^\circ\text{C}$

The amount of Cu incorporated into glass at 550°C increased with increasing time in the range of 10 min to 120 min

The glasses containing 10 mole percent or more Al_2O_3

showed the stepwise concentration profile which is usually characteristic of the ion-exchange under an applied field

The concentration of Cu found at the surface after a sufficient ions-exchange was found to be 11-15 wt % of glass corresponding to the replacement of 30-40% Na_2O by Cu_2O

The Al_2O_3 content markedly affected the ion-exchange rate. The presence of CaO in glass suppresses the Cu-Na ion exchange rate.

1 3 OBJECTIVE OF PRESENT INVESTIGATION:

Some recent work in this laboratory has shown that high electrical conductivity can be induced in certain oxide glasses containing aluminium dispersoids by subjecting them to a sodium \rightleftharpoons silver ion exchange treatment⁹. In the present work, a large concentration of aluminium metal has been induced and the resultant effect on the electrical properties of glasses is studied. The objectives of this investigation can therefore be summarised as follows:

- 1 To prepare the glass samples from reagent grade chemicals
- 2 To subject all the above glasses to a sodium \rightleftharpoons silver ion exchange under suitable conditions of temperature for reasonable period of time
- 3 To characterize the electrical properties of both virgin and ion exchanged glasses by complex impedance analysis
- 4 To explore the possibility of generating highly conductive state in the ion-exchanged samples of the above glasses in bulk form

Chapter - 2

EXPERIMENTAL TECHNIQUES

2.1 PREPARATION OF GLASS:

The glasses investigated in present study are prepared from reagent grade chemicals. Their composition are given in Table 2.1

Na_2O is introduced as carbonate, B_2O_3 as boric acid, Aluminium as Aluminium powder (99.9%) and other ingredients (SiO_2) as their respective oxides. Each glass batch of a given composition is weighed, mixed thoroughly with acetone, dried and melted in an alumina crucible in an electrically heated furnace. Temperatures of melting of these glasses are in the range of 1400°C - 1450°C . The glass melt is kept at this temperature for about 2 hours and is mechanically stirred to make it bubble free and homogeneous. The melt is poured in aluminium mould of dimensions $5\text{ cm} \times 1\text{ cm} \times 0.5\text{ cm}$ and is immediately transferred to the annealing furnace at 500°C where it is annealed for about 6 hours. The furnace is switched off and the glass is allowed to cool in the furnace to room temperature. The annealing treatment helps in removing strains induced in the glass due to thermal stresses and thus prevents cracking of the sample.

2.2 SAMPLE PREPARATION FOR ELECTRICAL RESISTIVITY MEASUREMENT:

The sample is prepared by polishing the glass piece using silicon carbide grit of different mesh sizes (100, 240, 320, 400, 600, 800 respectively) to the dimensions approximately

10 mm x 8 mm x 1.5 mm The gold is deposited by vacuum evaporation on two opposite surfaces of the larger dimensions after measuring the cross-sectional area and thickness of the sample with a micrometer (MITUTOYA MAKE)

2.3 CONDUCTIVITY CELL:

Fig. (2.11) shows the schematic diagram of the cell used for electrical measurements. It consists of a stainless steel tube of about 300 mm length and of 50 mm diameter. The tube has a cooling coil assembly attached to its top. The main structure i.e. the sample holder can be fitted within the jacket.

The main structure of the cell consists of two stainless steel rods fixed to a bronze flange which act as two electrodes (E_1 & E_2). Each rod is brazed to a rectangular stainless steel plate so that the sample can be sandwiched between the two plates. Both the electrodes have spring arrangements so that they can be moved up and down. The lower electrode is supported on an alumina substrate which itself is attached rigidly to the main structure. A chromel-alumel thermo-couple is placed near the electrode assembly, its other end taken out through the teflon disc fitted into the flange. There is a central rod in the main structure which can be connected to ground. Also the electrodes are shielded by Fig. (2.11) metal shielding.

The whole assembly can be used for the temperature

range from room temperature to 500°C with an accuracy of $\pm 1^\circ\text{K}$

2 4 RESISTIVITY MEASUREMENT COMPLEX IMPEDANCE ANALYSIS OF A.C. DATA

The schematic diagram for the circuit used in Fig

(2 2 2)

A General Radio GR 1615 transformer ratio arm capacitance bridge with GR 13136 oscillator bench and GR 1232 tuned amplifier and null detector are used to measure capacitance C and the loss factor $\tan \delta$ at various frequencies and at various temperatures.

The frequency range used is from 100 Hz to 100 K Hz and measurements carried out over a temperatures range from Room Temperature to 300°C. The real and imaginary parts of complex impedance can be calculated by using the values of $\tan \delta$ and the capacitance $C(\omega)$. The complex impedance is given by (43)

$$Z^* = Z' - i Z'' = \frac{G}{G^2 + \omega^2 C^2} - i \frac{\omega C}{G^2 + \omega^2 C^2} \quad (2 1 5)$$

$$\text{Hence, } Z' = \frac{G}{G^2 + \omega^2 C^2} \quad (2 2 6)$$

$$\text{and } Z'' = \frac{\omega C}{G^2 + \omega^2 C^2} \quad (2 3 7)$$

where G is the conductance and $G = \omega C \tan \delta$

The capacitance and $\tan \delta$ values are measured for various frequencies and for various temperatures and the

values of Z' and Z'' can be calculated using equations (215), (226) & (237)

For a fixed temperature the values of Z' & Z'' can be calculated for different frequencies from the corresponding C and $\tan \delta$ values. Complex impedance plots are made from these data

The plot is usually a semicircle passing through the origin. The intersection of the plot on the Z' axis is measured which gives the value of dc resistance. The resistivity can be calculated by knowing the dimensions of the specimen i.e.

$$\rho = R_{dc} \frac{l}{A} \quad (248)$$

where l = length, A = area of cross section of the electrode (gold plated)

The $\log(\rho)$ vs $\frac{1}{T}$ is plotted, which is a straight line and the value of activation energy can be calculated from the slope of the line.

2.5 X-RAY ANALYSIS:

'Rich Seifert 2002D Isodebyeflex Diffractometer' with Cu $K\alpha$ (wave length = 0.291 nm) radiation has been used to record the X-ray diffraction pattern of the glass samples at the scanning speed of 3° per minute. The glass samples are ground to a very fine powder in an agate mortar.

The interplanar spacings have been computed from the X-ray diffraction diagram using the well known Bragg's relation:

$$2d_{hkl} \sin \theta = \lambda \quad (259)$$

where d_{hkl} = interplanar spacing

θ = diffraction angle

λ = wavelength of the radiation used

The calculated d_{hkl} values are compared with the existing data of various possible phases

2.6 ELECTRON MICROSCOPIC ANALYSIS BY TEM:

2.6.1 SAMPLE PREPARATION:

For microstructural examination the carbon support films are initially prepared by vacuum evaporation technique on a precleaned glass slide. The carbon films are then cut into small squares and made to float on the surface of distilled water in a crystallization dish. These small portion of films have been subsequently fished out with copper grids such that they rest on the matte side of the grid for better adhesion. The carbon film not only holds the glass particles but also serves to conduct the heat produced due to interaction of electron beam with the sample.

The glass sample is thoroughly ground in an agate motor, dispersed in acetone and then allowed to settle. The

process makes thick particles to settle on the bottom layer of the container while leaving very fine particles in suspension. A drop of acetone containing finely dispersed glass particles is then poured on the grid containing carbon film. The acetone evaporates leaving the fine powder of glass on the grid. One drop of collodion (0.5 wt % solution in amyl acetate) is poured in distilled water to form a very thin film of collodion. The carbon coated grids containing glass particles are then placed on this film such that the particles face the collodion film. Now the grids are fished out by clean glass slide. In doing so, glass particles are sandwiched between carbon and collodion films. The collodion coating keeps the particles in fixed position and also prevents them from falling into the sample chamber during examination.

Microstructural details of glass sample has been examined in a Phillips EM 301 Transmission Electron Microscope Operated at 100 KV. The selected area diffraction patterns are recorded.

In order to identify the precipitated phase in the sample radii of the diffraction range have been measured from the negative by using a graduated eye piece with an accuracy of 0.1 mm. The interplanar spacings are calculated from the relation given below:

$$\text{Camera Constant} = r \cdot d_{hkl} \quad (2.6.10)$$

where r = radius of the diffraction ring

d_{hkl} = interplanar spacing of the (hkl) plane giving rise to diffraction ring

The value of camera constant has been determined from the diffractions pattern of a gold sample taken as standard under identical condition. Once the phase is identified, actual camera constant is calculated by considering the most prominent indexed line of that particular diffraction pattern and the corresponding reported values of d spacings. The camera constant calculated in this manner is used to calculate the d_{hkl} values of the other rings present in the diffraction pattern. This procedure gives the accurate value of camera constant and hence the d_{hkl} values.

2.7 DENSITY MEASUREMENT:

Density of glass is measured by liquid displacement method. A known weight W_1 of glass is dipped into toluene (density = 0.87 gm/cc) and weighed giving its value W_2 . Density is calculated by the following formula

$$d = \frac{W_1}{W_1 - W_2} d_1 \quad (2.7.11)$$

where d_1 = density of toluene

2.8 DIFFERENTIAL SCANNING CALORIMETRY (DSC)

A Dupont 910 DSC is used for thermal analysis of the powder sample of different glass compositions. The powdered samples are put in small aluminium pan provided by the manufacturer to use as crucible. A second empty Al pan is used as a reference. The heating cycle in the DSC for example, the

initial temperature, final temperature, rate of heating, minutes in isothermal etc are programmed. The specimen is first heated to 400°C at a rapid rate and is brought to a stand by position. From this temperature the specimen is heated at a rate of 10°C per minute to the final temperature of 600°C. On the D S C and the recorder system measurements can be made in different sensitivities.

Two sensitivity ranges IX and X are available in D S.C. The chart recorder sensitivity can be chosen from 0.11 and 10 volt full scale reading. For the experiment IX D S.C. sensitivity and 0.1 volt chart recorder sensitivity are used. The measurements are made in D S C calibrated mode of the equipment. Base line adjustments are made at the start of the set of experiments but no adjustments are made in between to avoid the change in D S C peak characteristic. The two-pen change recorder is used to record against time, Q , Q being the heat evolved or absorbed and T , the temperature. The typical experimental conditions used are shown as below:

Heating rate	= 10°C/min
Initial temperature	= 400°C
Final temperature	= 600°C
Range for Q	= 0.1 V
Range for T	= 0.1 V
D S.C. sensitivity	= IX
D S C in calibrated mode	

2.9 ION-EXCHANGE:

All the glass compositions are ion exchanged by dipping

them in a molten bath of silver nitrate. In this process the sodium ions are exchanged by the silver ions in the glass sample upto a certain thickness.

2 10 SAMPLE PREPARATION FOR ION-EXCHANGE.

The glass sample is polished to the dimension of about 2mm x 2mm x 2 mm by using silicon carbide grits of different mesh sizes (100, 200, 320, 400, 600, 800)

Then the sample is kept in a pyrex tube containing molten AgNO_3 at 300°C in an electrically heated furnace for 48 hours. After the ion-exchange is over, the sample is taken out, washed and boiled to remove the excess AgNO_3 .

For electrical resistivity measurement, on the ion exchanged glass sample, the gold is deposited by vacuum evaporation on the two opposite surfaces after measuring the cross-sectional area and thickness of the sample with a micrometer (MITUTOYA MAKE)

The electrical resistivity measurements/complex impedance analysis of A C data is done exactly in the same manner as for the virgin glasses.

Chapter - 3

RESULTS AND DISCUSSION

3 1 Transmission Electron Microscopic Analysis:

3 1 1 MICROSTRUCTURE

Fig (313) represents the micrograph of the glass sample No A2. The electron micrograph shows the dispersion of a dark phase in light matrix. The dark regions comprise of aluminium particles. The aluminium particles have a range of dimensions from 22 nm to 144 nm.

3 1 2 SELECTED AREA DIFFRACTION:

Fig (324) shows the SAD of gold film. Table (312) gives the data obtained from the Fig (324). The diameters of the diffraction rings have been measured and the value of the camera constant has been calculated and is given in Table (312).

The selected area diffraction of glass sample A2 (containing 10 mole percent of aluminium) has been shown in Fig. (335) which contains two diffraction rings. The diameters of both the diffraction rings have been measured and rings are identified by using the camera constant obtained from the gold film. Table (324) gives the diameter and d_{hkl} value for glass No A2. It has been found that the two rings in the SAD of sample A2 belong to the (111) and (200) planes of aluminium. Table (335) gives the comparison of d_{hkl} values of aluminium with those obtained from the SAD of glass No A2.

3 2 DIFFERENTIAL SCANNING CALORIMETRY:

Fig (346) gives the Q versus T plots for different glass samples. The value of glass transition temperature⁴⁴ have been found out and is given in Table (345)

3 3 X-ray ANALYSIS:

Fig (357) to Fig (3810) give the X-ray analysis for different glass samples. A broad peak is found in each plot which is characteristic of an amorphous material. The X-ray analysis is not able to detect the presence of metallic aluminium granules.

3 4 DENSITY OF THE GLASSES

The densities of the different glass samples have been measured by liquid displacement method. The values are given in Table (211)

3 5 AC MEASUREMENT AND COMPLEX IMPEDANCE ANALYSIS.

A C measurement yields the value of conductance (G) and capacitance (C) as a function of frequency. The impedance analysis have been carried out for all glass samples at various temperatures ranging from room temperature to 300°C. The frequency has been varied from 100 Hz to 100 K Hz.

The various points in the $Z' - Z''$ plot are found to lie on a semicircle starting from the origin. The intersection of the semicircle on the real (Z') axis yields the D C resistance (R_{dc}) of the sample. Figures (3911) to (31618) are typical $Z' - Z''$ plots for the different glass samples.

It is clear from the $Z' - Z''$ plots that the value of D C resistance and hence the D C resistivity is decreasing as the mole percent of metallic aluminium is increased. Such changes in resistivity values may be due to the phase structure in these glasses which increase the mobility of the alkali ions.²⁸ According to this model, the sodium ions migrate along the interface between the alumina-rich and alumina-deficient glass phases.³¹

3.6 TEMPERATURE DEPENDENCE OF RESISTIVITY.

Fig (3.17.19) to (3.28.30) show the variation of $\log \rho$ against $\frac{1}{T}$ for all glass samples. For each sample the plot has been drawn for various temperatures indicating the temperature dependence of resistivity. The temperature dependence of resistivity is found to obey the Rasch-Hinrichsen equation³⁷

$$\rho = \rho_0 \exp \left(\frac{Q}{KT} \right) \quad \dots (3.1.12)$$

Where ρ_0 is the preexponential factor and Q is the activation energy. Table (3.5.13) summarises the values of Q and ρ_0 for all the glass samples including the ion-exchanged ones.

Figure (3.25.27) gives a comparison of the resistivity variation with temperature for the different glasses studied.

Figure (3.26.28) to (3.28.30) give the $\log \rho$ versus $\frac{1}{T}$ plot comparing the values for the glass numbers A1 and IA1, A2 and IA2, A3 and IA3 respectively. ~~as the~~ ~~resistivity~~ ~~is~~

in the virgin as well as the ion-exchanged states. The values of activation energy and the pre-exponential factor have been given in Table (3.5.3.6). Fig (3.18.20) for the glass containing 10 mole percent of aluminium shows two regions in the curve with different values of activation energies. The low temperature part of the curve is believed to arise due to alkali ion migration. The mechanism responsible for the rather high value (2.7 eV) of activation energy exhibited by the glass No. A2 in the high temperature range is not understood at this stage. More systematic analysis of the resistivity of these glasses at different electric fields may clarify whether the above effect is due to some kind of switching phenomenon or not.²⁹

The two portions in the $\log \rho$ vs $\frac{1}{T}$ curve for glass no. A3 (glass containing 15 mole percent Al) can be explained in the following manner. The low activation energy (viz., 0.1 eV) part is believed to arise due to electron tunneling between the metallic granules of aluminium whereas the higher activation energy part is due to ionic migration. The latter value is higher than that exhibited by glass No. A2 (glass containing 10 mole percent of Al). This may be due to a higher concentration of Al_2O_3 present in the glass matrix of A3 due to the oxidation of aluminium particles during the glass melting operation. However at this stage, the possibility of a switching mechanism of the type mentioned above can not be ruled out [Fig. 3.19.21]

It is interesting to note that in glass no. A4 the ionic migration of sodium ions only controls the activation

energy It is likely that in this system the effective concentration of Al_2O_3 in the glass matrix is higher than that in glass No 13 As a consequence, the inter-island separation between the metallic aluminium granules is higher in this system than that of A3 The electron tunneling mechanism thus makes a negligible contribution to the conductivity of the sample ⁴⁶(Fig 3 20 22)

For the ion-exchanged samples the values of activation energy are slightly lower than those for virgin glasses This is due to the fact that the silver particles should have a lower activation energy than sodium ions ⁴⁶

Figure [3 21 23] to [3, 24 26]

The ion-exchanged sample of glass No A2 shows a drastic reduction in the resistivity values as compared to those of the virgin glass Evidently the microstructural features in the ion-exchanged layer of this glass are conducive to the formation of an interconnected silver rich phase possessing high electrical conductivity ⁴⁶ It is however, to be emphasized that the other glasses may also exhibit this type of switching A systematic study of voltage-current characteristics under D C field will be able to throw light on this problem

3 7 ϵ' VERSUS LOG f PLOT:

In Fig (3 293) to (3 323A) ϵ' versus log f plots have been shown for various temperatures It can be seen from these plots that the value of ϵ' increases with increasing

mole percent of aluminium within the glass This is believed to arise due to space charge polarization⁴⁷

Table 211

Composition of the Glasses:

S No	Glasses	Composition in mole percent				Density g/cc
		Na ₂ O	B ₂ O ₃	SiO ₂	Al	
1	A1	25	10	65	-	2.55
2	A2	25	10	55	10	2.98
3	A3	25	10	50	15	2.16
4	A4	25	10	45	20	2.52

Table - 312

SAD of the Gold Film for the Calculation of Camera Constant
(Lattice parameter $a = 4.0786 \text{ \AA}$)

S No	Diameter of diffraction rings (mm)	radii of the diff- raction rings R mm	hkl	d_{hkl} \AA	Camera constant $d_{hkl} R$ mm \AA	Camera const (average mm \AA)
1	7.1	3.55	111	2.36	8.38	
2	8.1	4.05	200	2.05	8.30	
3	11.8	5.9	220	1.44	8.49	8.45
4	13.9	6.95	311	1.23	8.54	
5	14.4	7.2	222	1.17	8.42	
6	18.4	9.2	331	0.93	8.56	
7	18.8	9.4	420	0.90	8.46	

Table - 323

SAD of the glass sample A2 Calculation of d_{hkl} values

S No	Diameters of the diffraction rings	radii of the diffraction rings (R_s)	$d_{hkl} (\text{\AA})$ = Camera Constant R_s
1	7.5	3.75	2.26
2	7.8	3.9	2.17

Table - 334

Comparison of d_{hkl} values of Aluminium with those obtained from SAD of glass sample A2 (glass containing 10 mole percent of Al)

S No	hkl	d_{hkl} (Al)	d_{hkl} calculated
		A S T M	A°
		A°	
1	111	2 34	2 26
2	200	2 02	2 17
3	220	1 43	
4	311	1 22	

Table - 345

Glass Transition Temperature (T_g)⁴⁴ for the
glass system

S No	Glass	T_g (°C)
1	A1	505°C
2	A2	520°C
3	A3	536°C
4	A4	480 5°C

Table - 356

Activation Energy (Q) and Pre-Exponential factor (ρ_0)
For The Glass System

S No	Glass	Q eV	ρ_0 ohm cm
1	A1	0.4	5.6×10^2
2	A2	0.5	7.4
3	A3	0.1 ^a	5.5×10^2
4	A4	0.4	3.4

a: Q = 0.1 eV in low T region

Q = 0.9 eV in high T region

Table - 36

Activation energy (Q) and Pre-exponential factor (ρ_0) for the ion exchanged glasses

S No	Glass	Q°	ρ_0
1	I A1	0.4	1.1×10^2
2	I A2	0.2	7.1
3	I A4	0.3	14.3

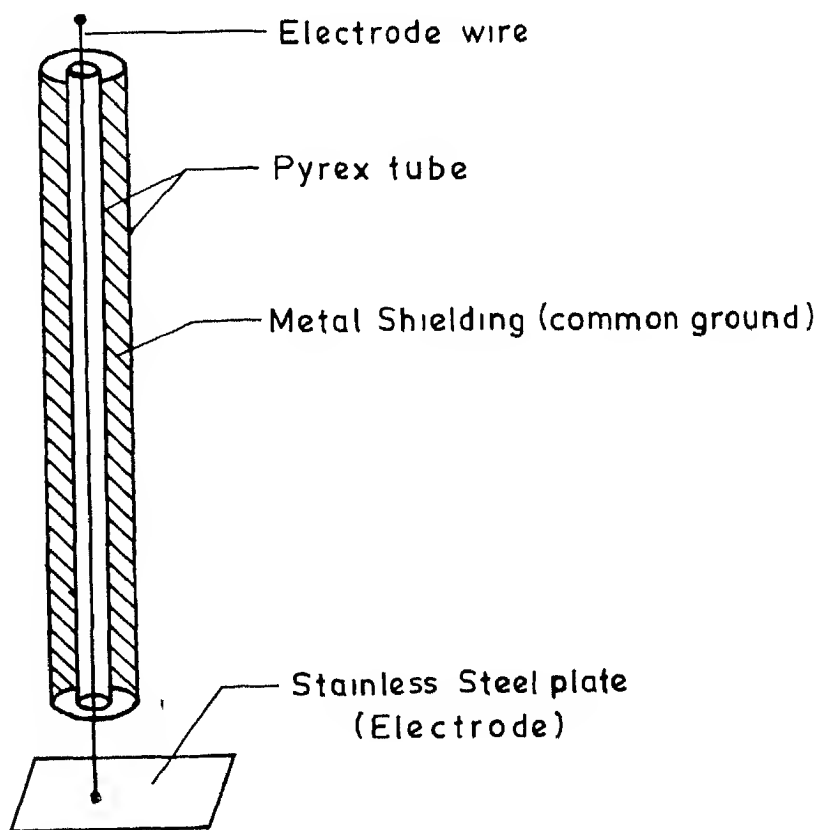
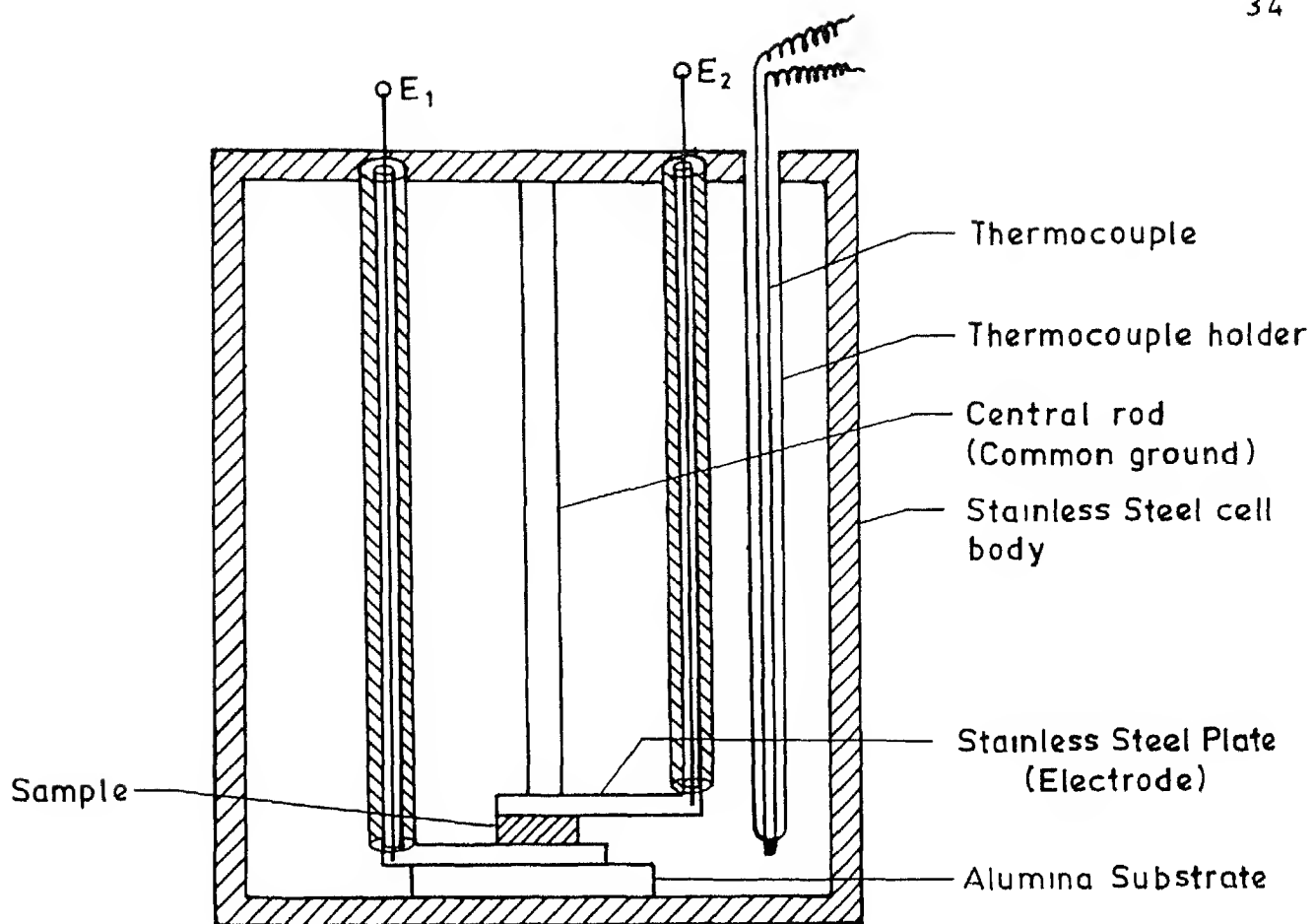


Fig 211 Schematic view of the conductivity cell

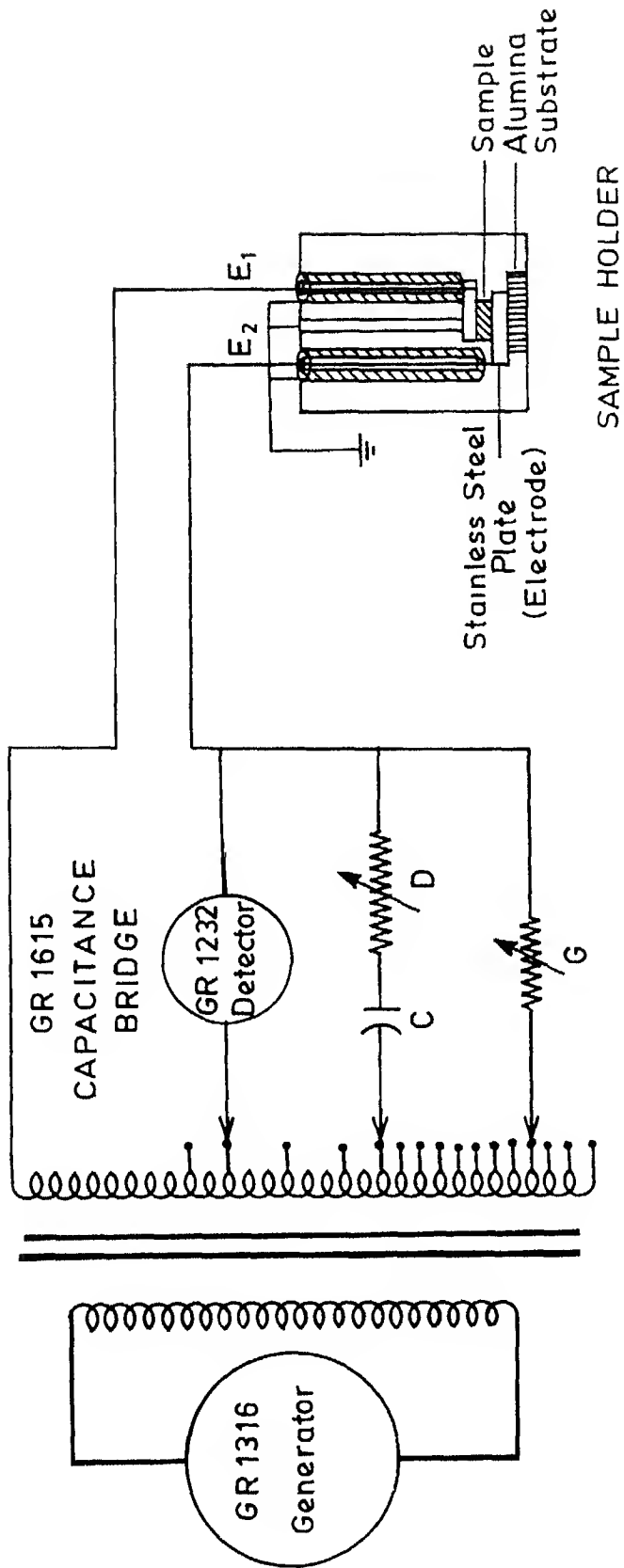


Fig 2 2 2 Schematic circuit diagram for A C resistivity measurement

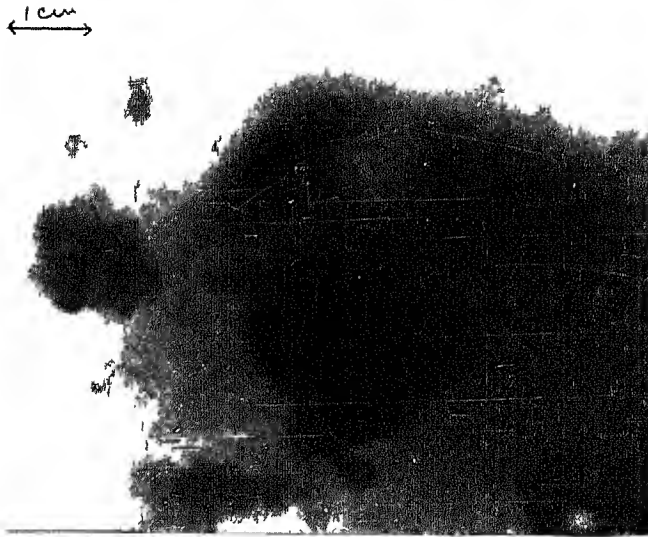


Fig. 3.1.3 Electron Micrograph of Glass
Sample A2 X 181730

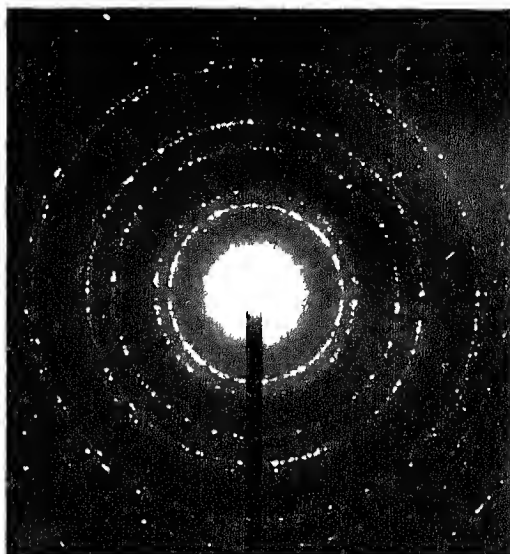


Fig. 3 2.4: Electron Diffraction Pattern
of Gold Film.

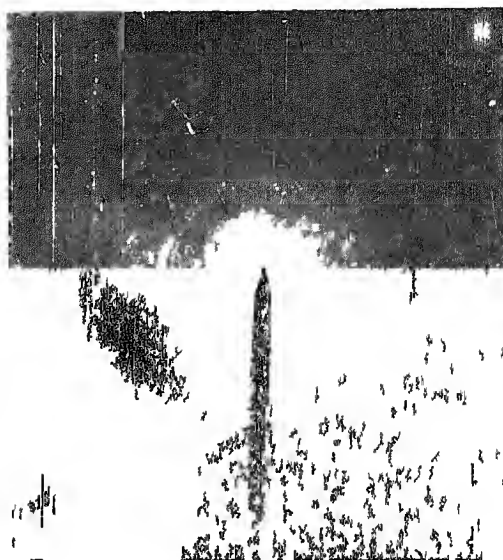


Fig: 3.3.5: Electron Diffraction Pattern
of the Glass Sample A2.

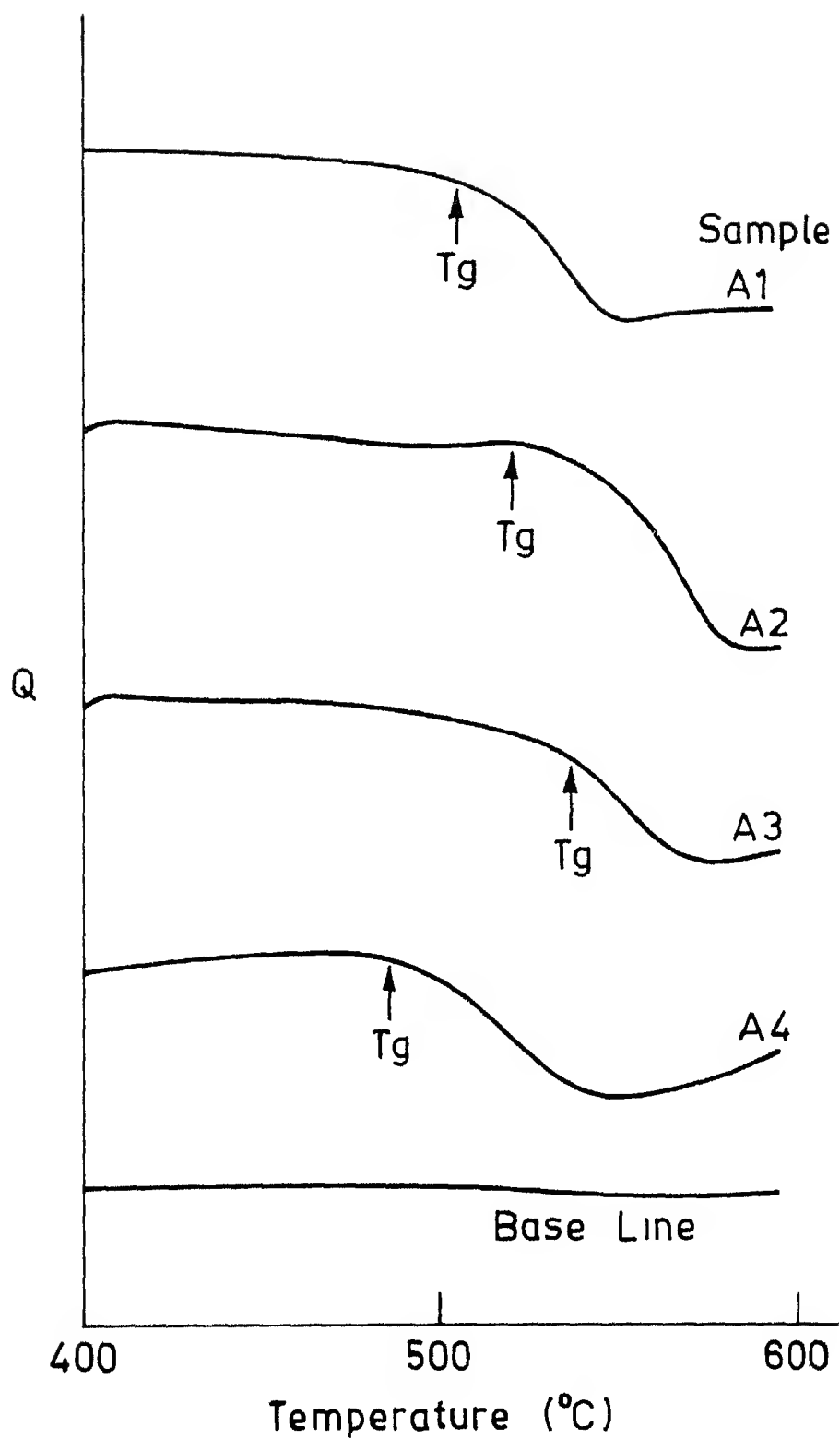


Fig 3 4 6 Differential Scanning Calorimetry for Different Glass Samples

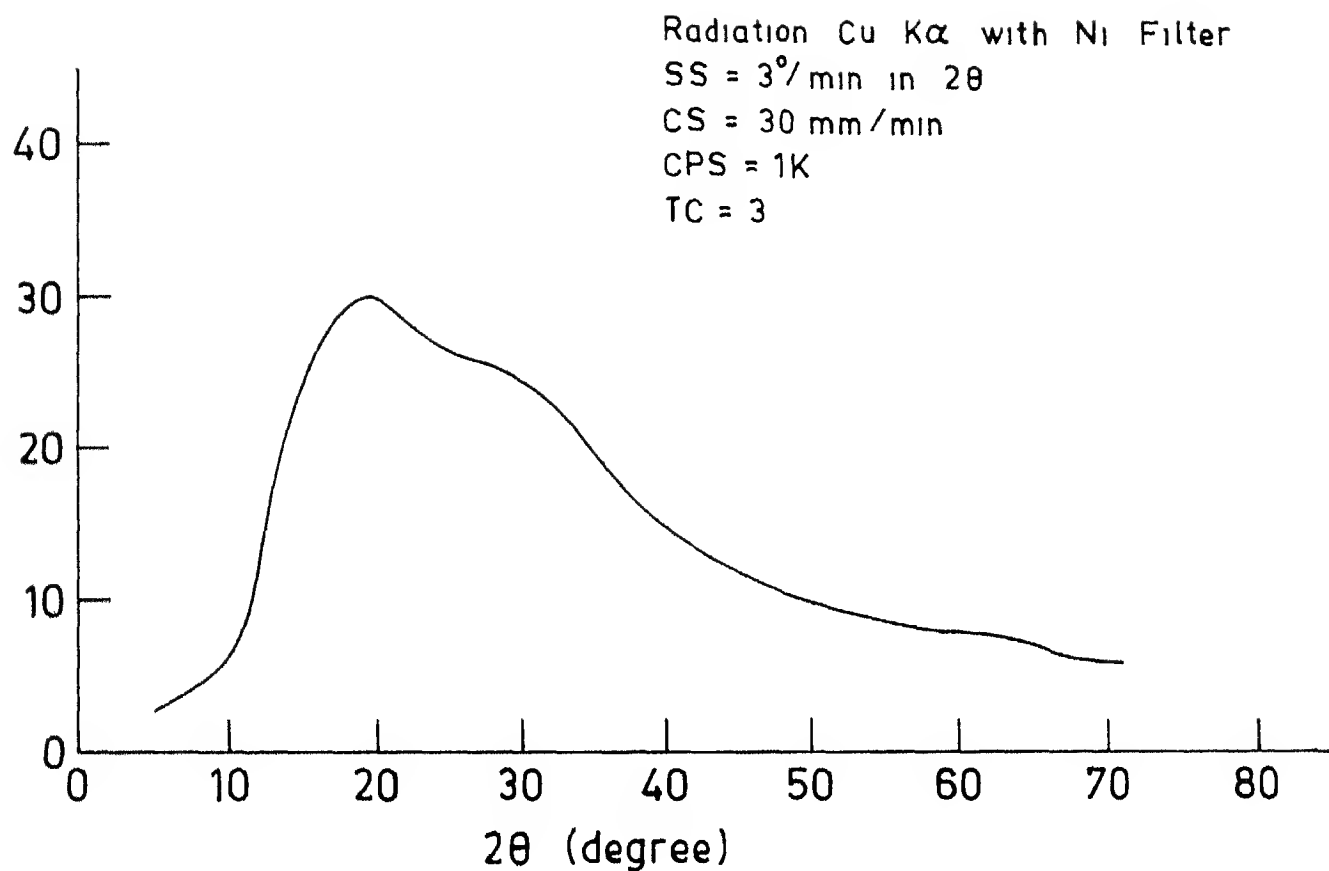


Fig 357 X-ray Analysis for Sample A1

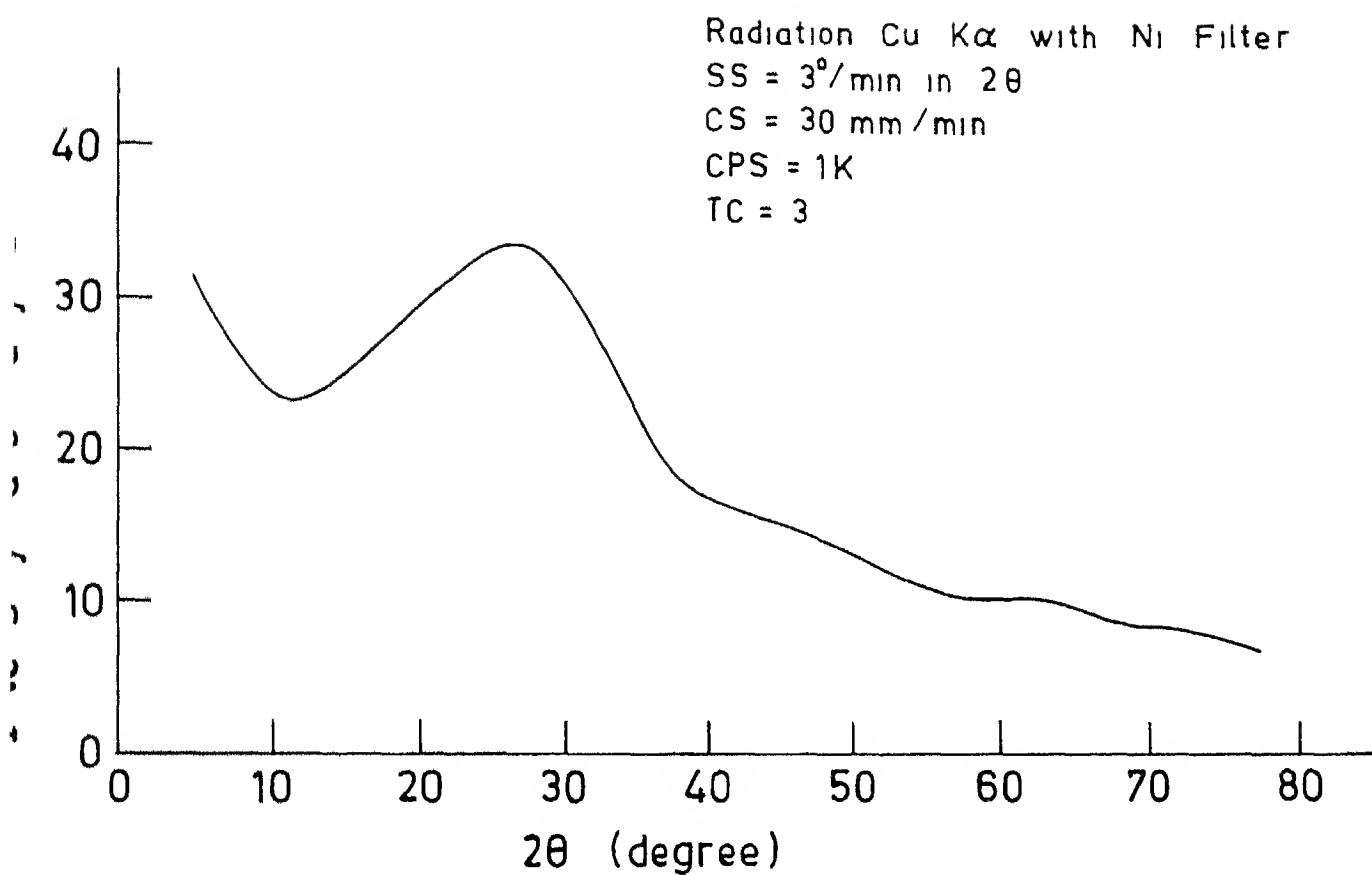


Fig 368 X-ray Analysis for Sample A2

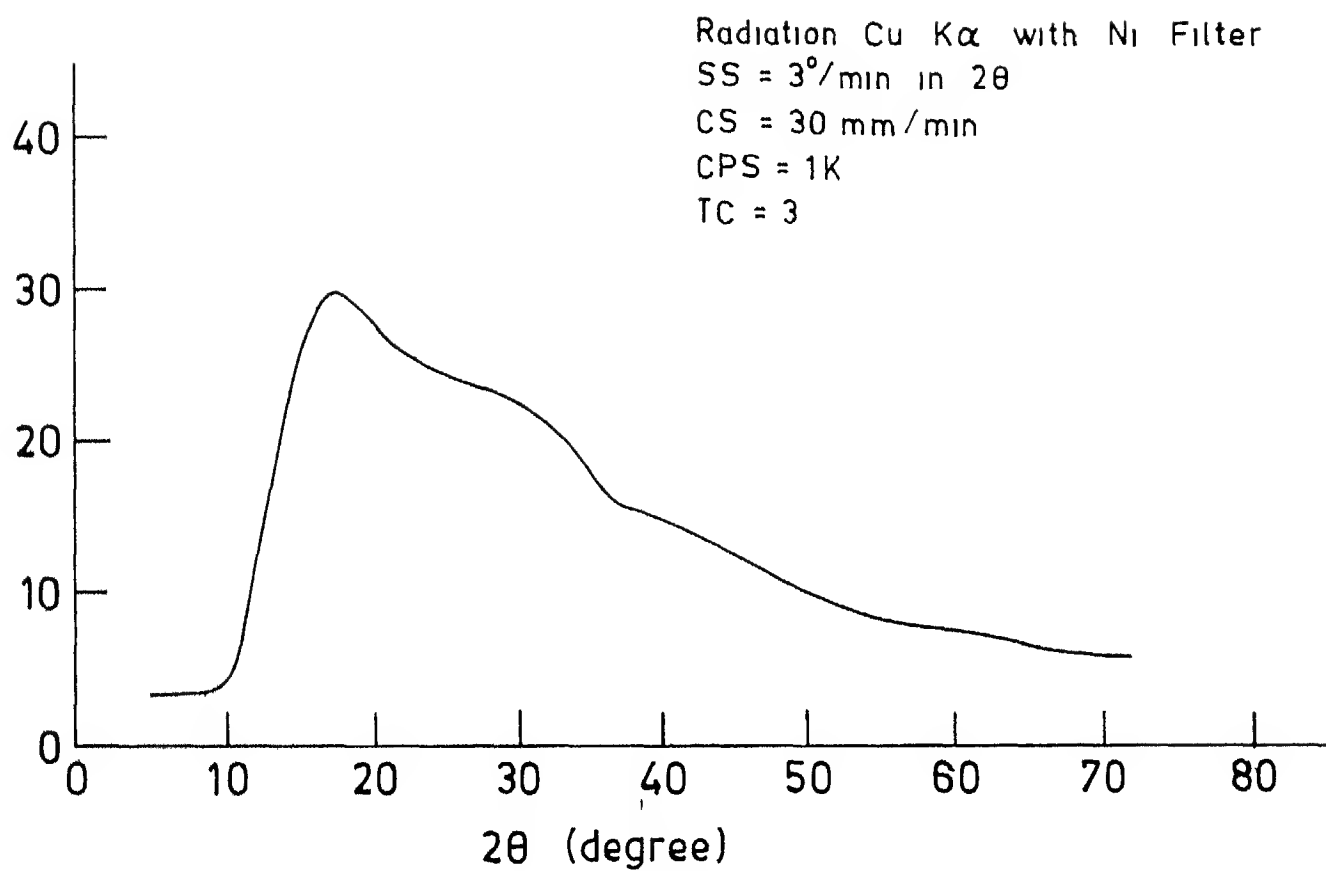


Fig 379 X-ray Analysis for Sample A3

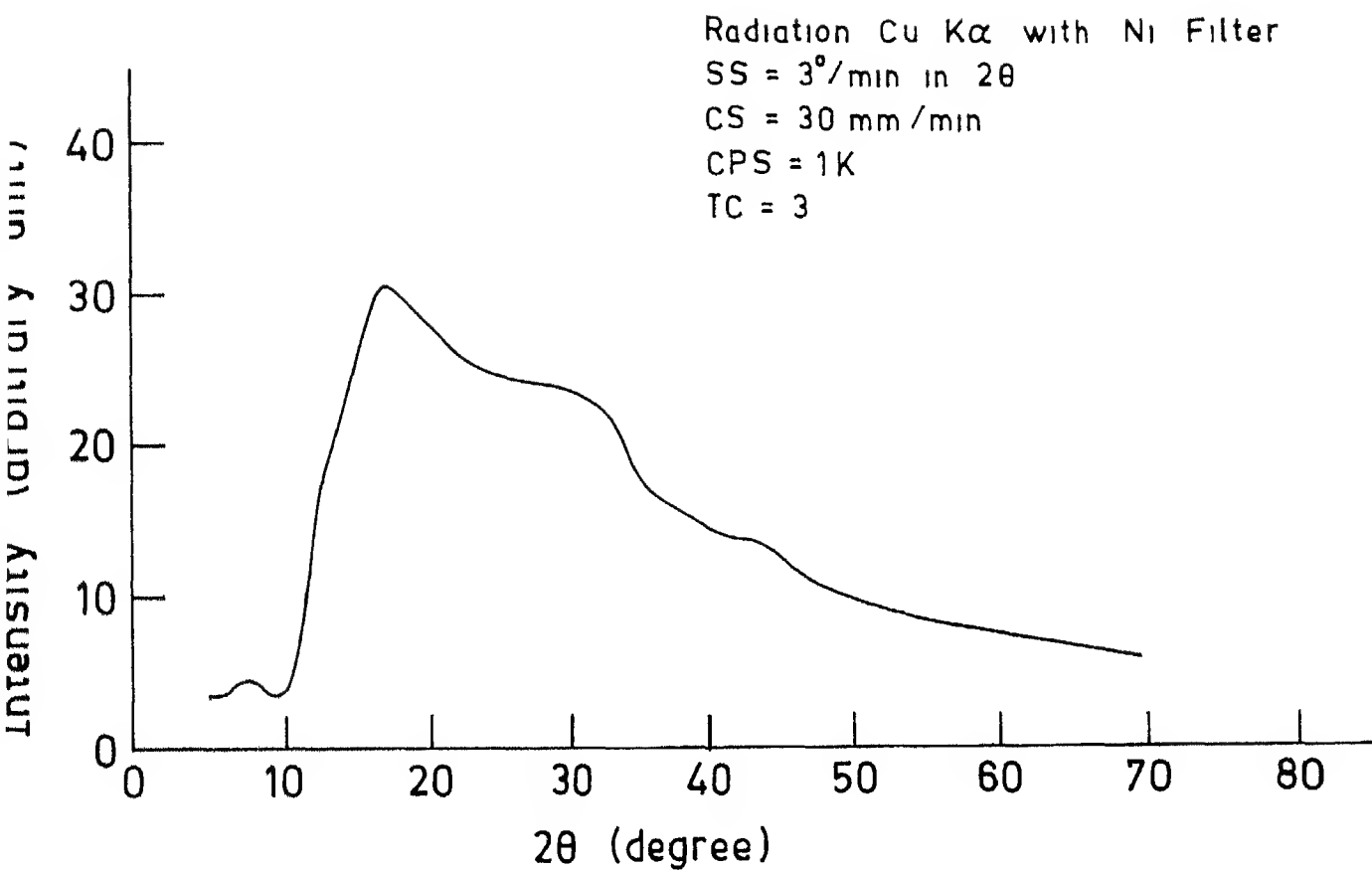


Fig 3 8 10 X-ray Analysis for Sample A4

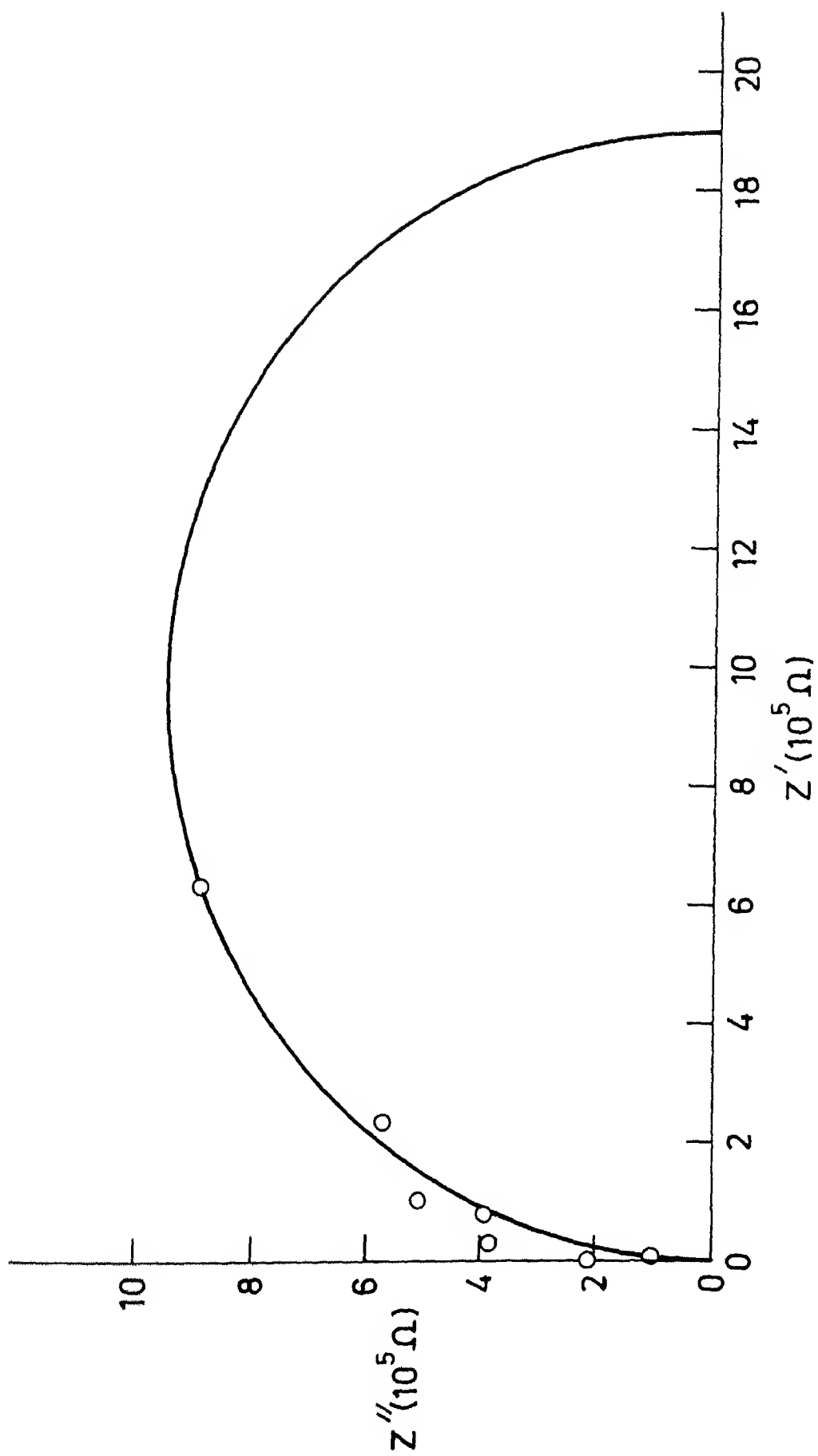


Fig 3911 Complex Impedance Plot for Glass Sample A1 ($T = 125\text{ }^{\circ}\text{C}$)

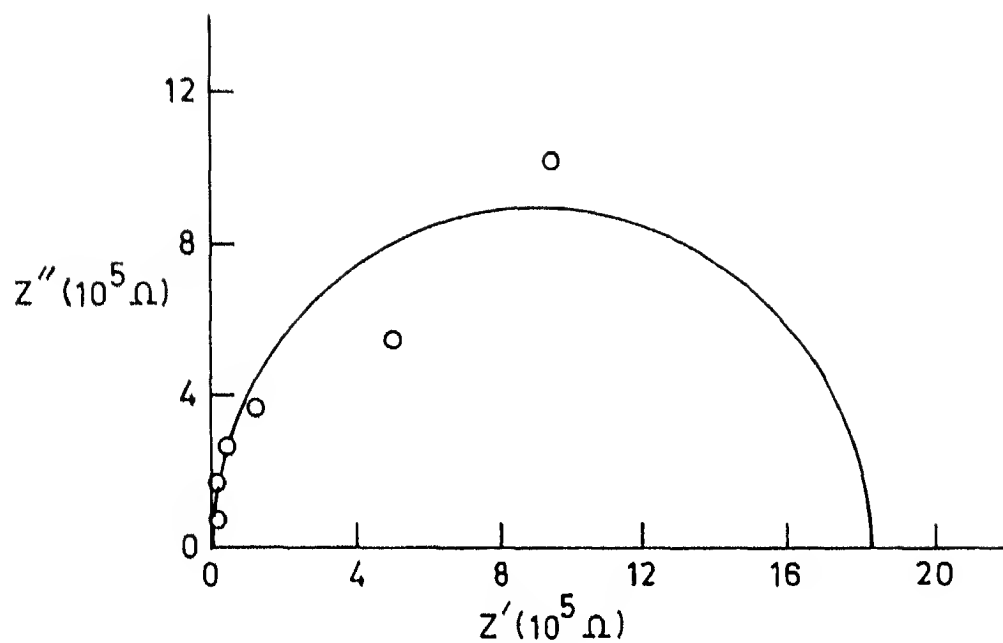


Fig 3 10 12 Complex Impedance Plot for Glass Sample A2 ($T = 100\text{ }^{\circ}\text{C}$)

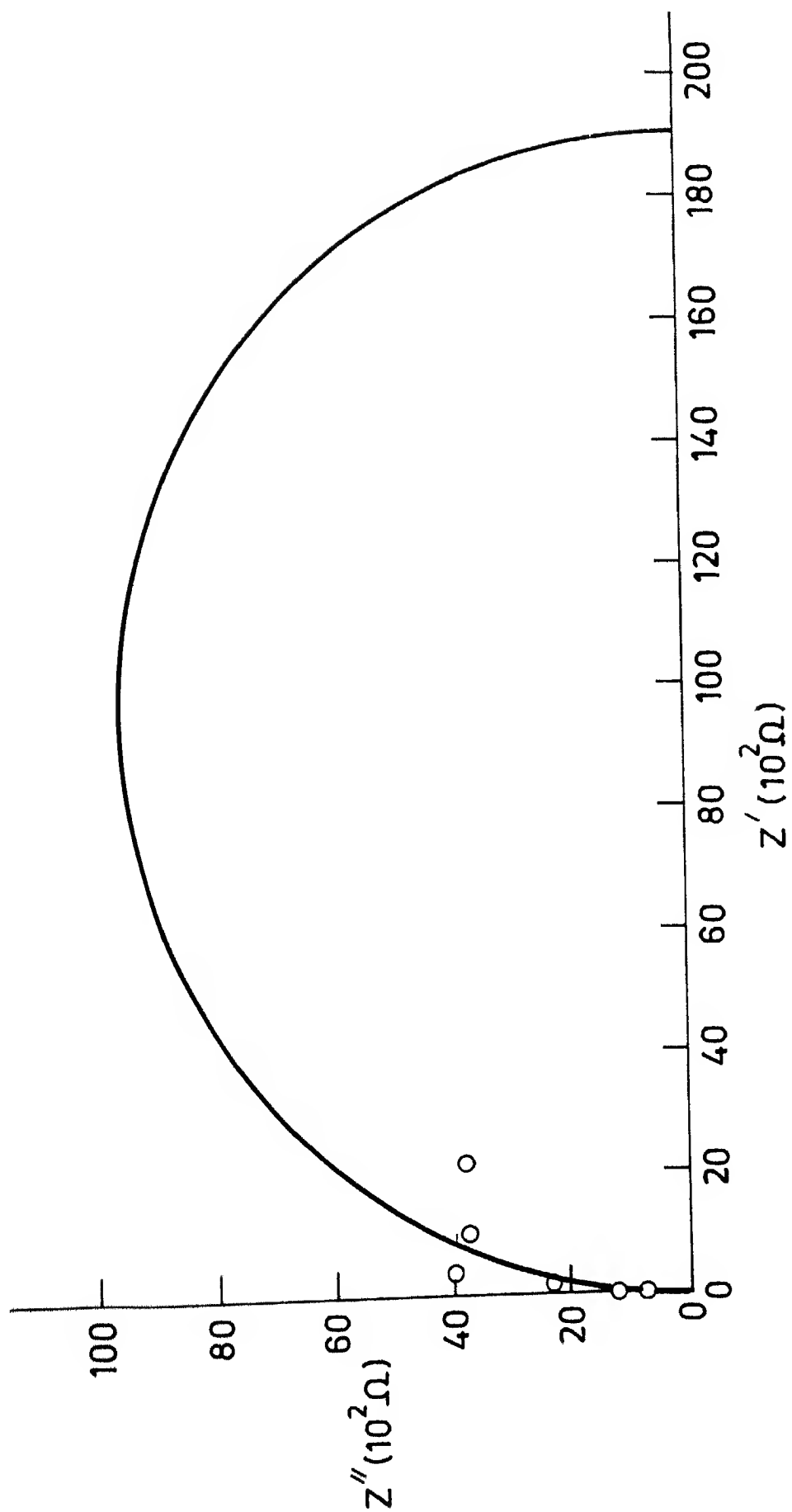


Fig 31113 Complex Impedance Plot for Glass Sample A3 ($T = 103\text{ }^{\circ}\text{C}$)

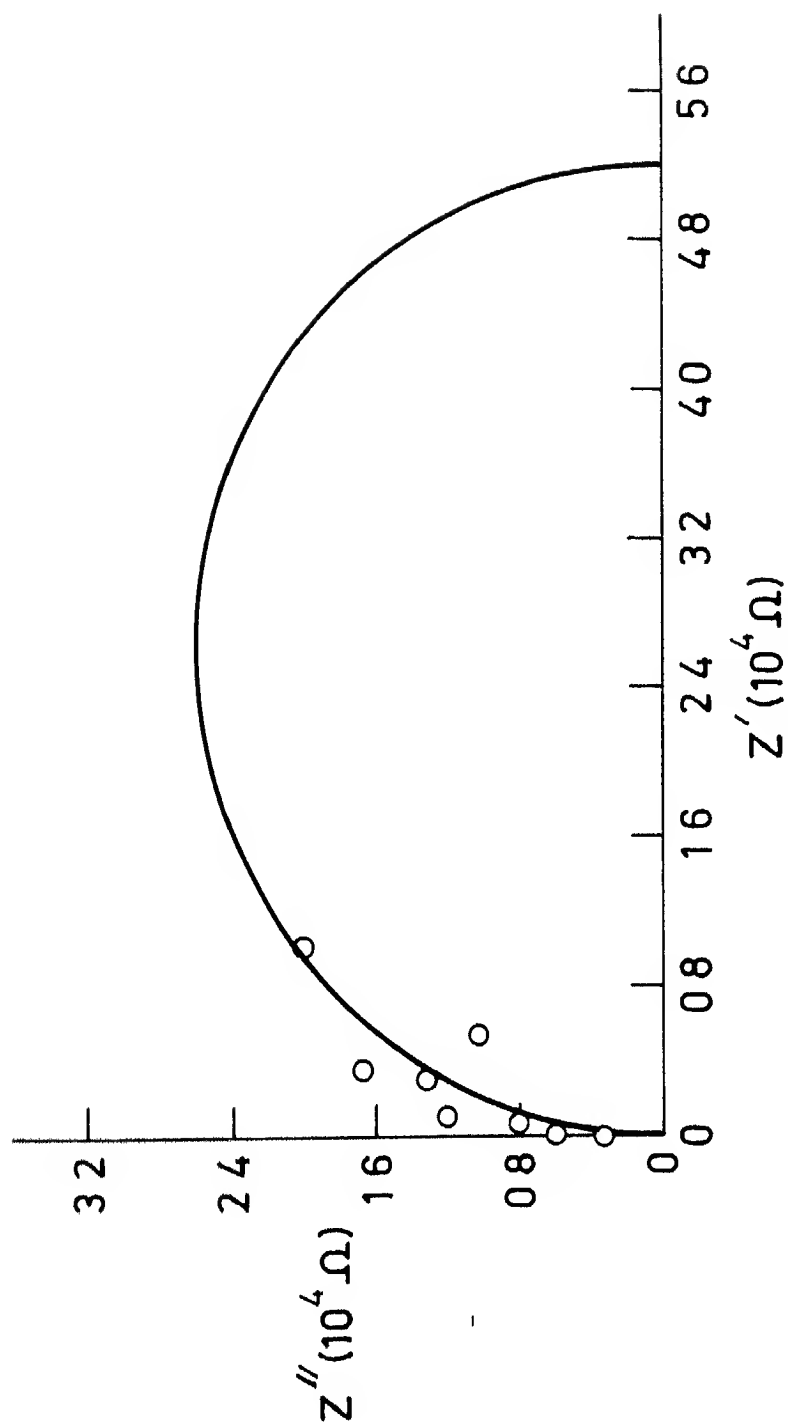


Fig 3 12 14 Complex Impedance Plot for Glass Sample A4
($T = 175\text{ }^{\circ}\text{C}$)

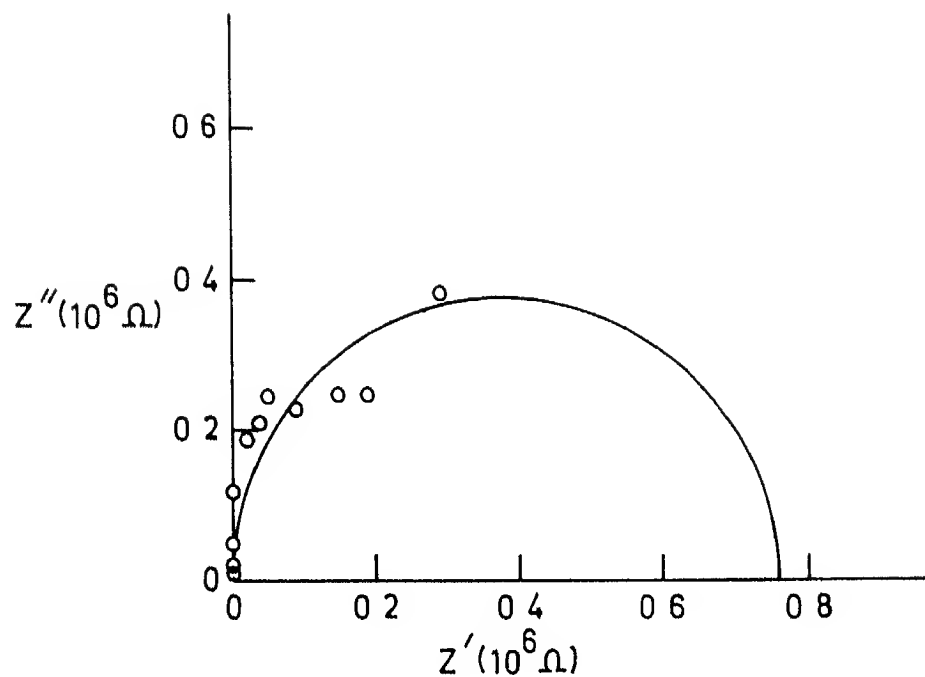


Fig 31315 Complex Impedance Plot for Glass Sample IA1 ($T = 303^\circ\text{C}$)

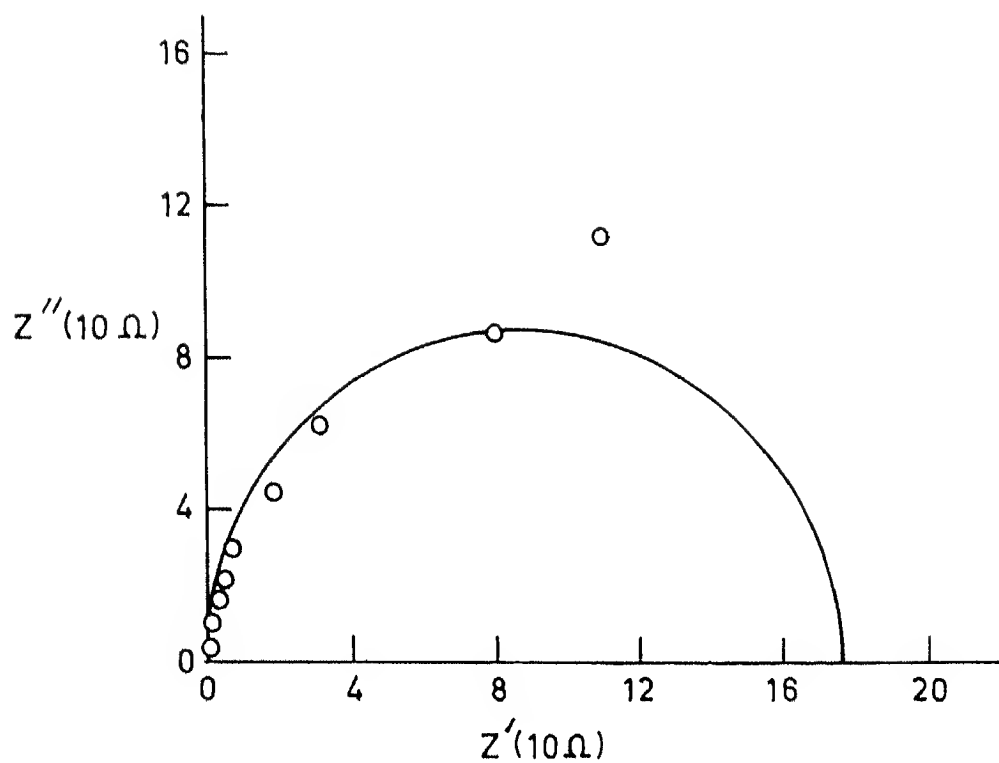


Fig 31416 Complex Impedance Plot for Glass Sample IA2 ($T = 191^{\circ}\text{C}$)

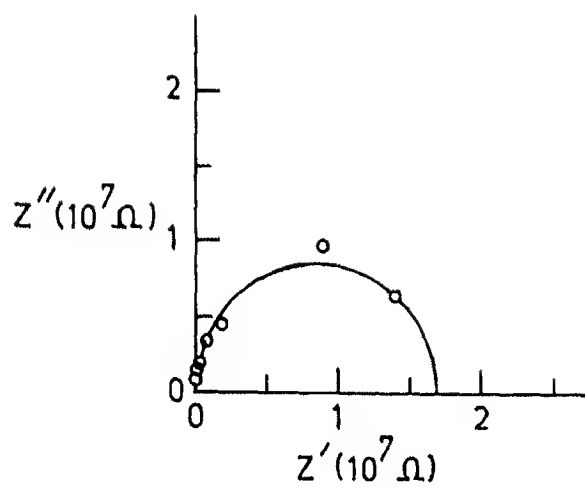


Fig 3 15 17 Complex Impedance Plot for
Glass Sample IA3 ($T = 80^\circ\text{C}$)

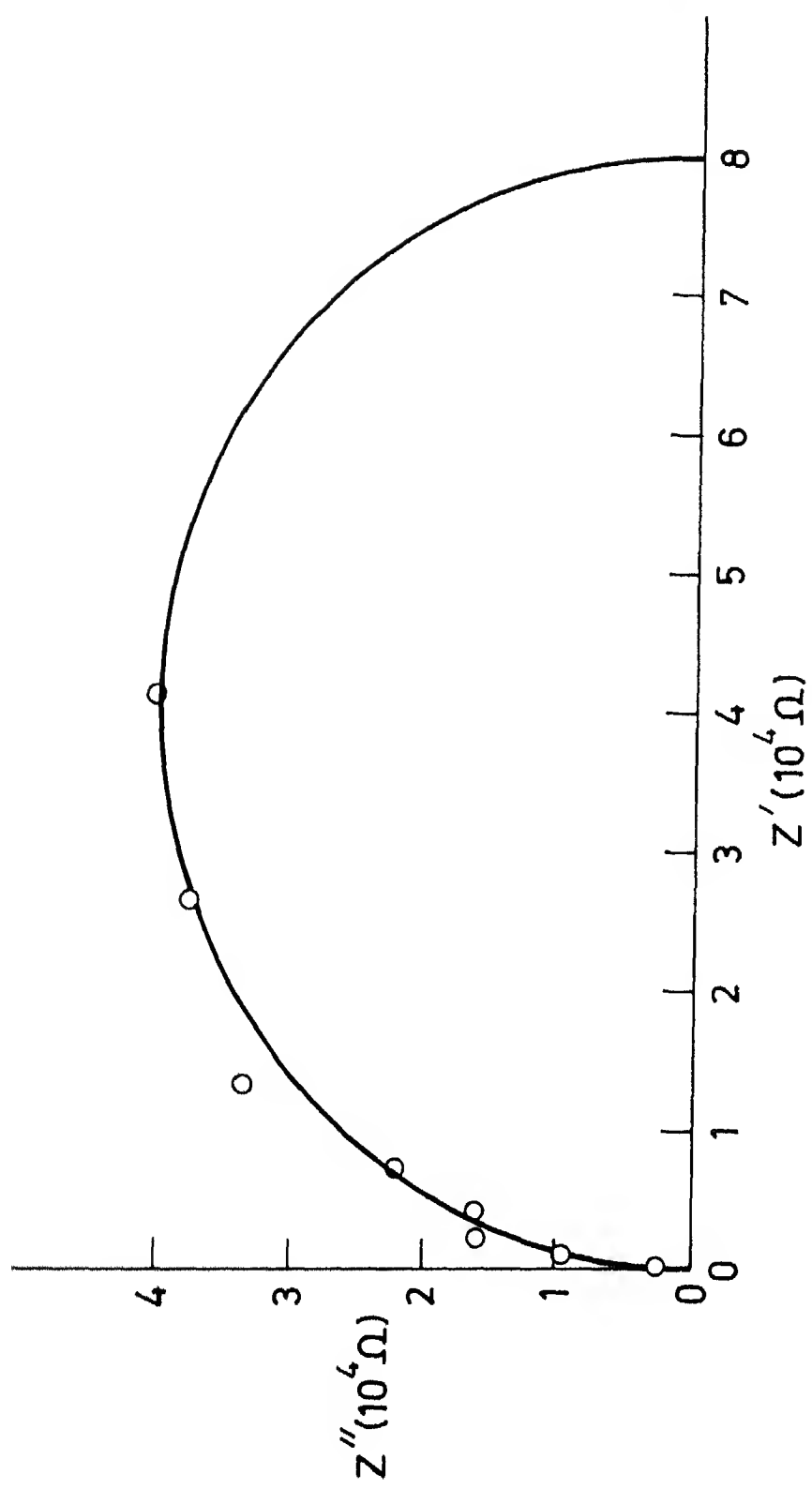


Fig 3 16 18 Complex Impedance Plot for Glass IA4 (T = 230 °C)

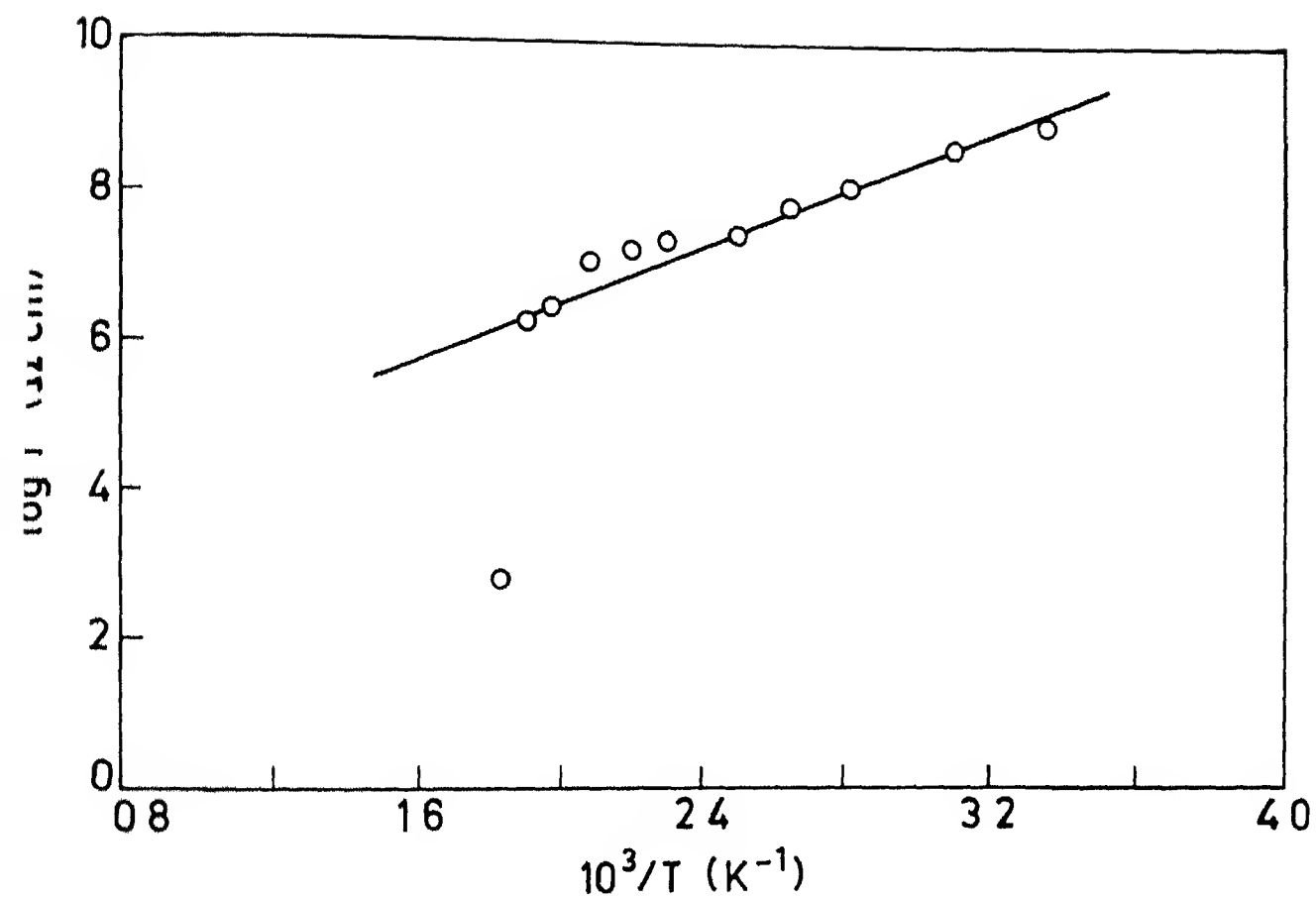


Fig 3 17 19 $\log P$ versus $1/T$ plot for glass sample A1

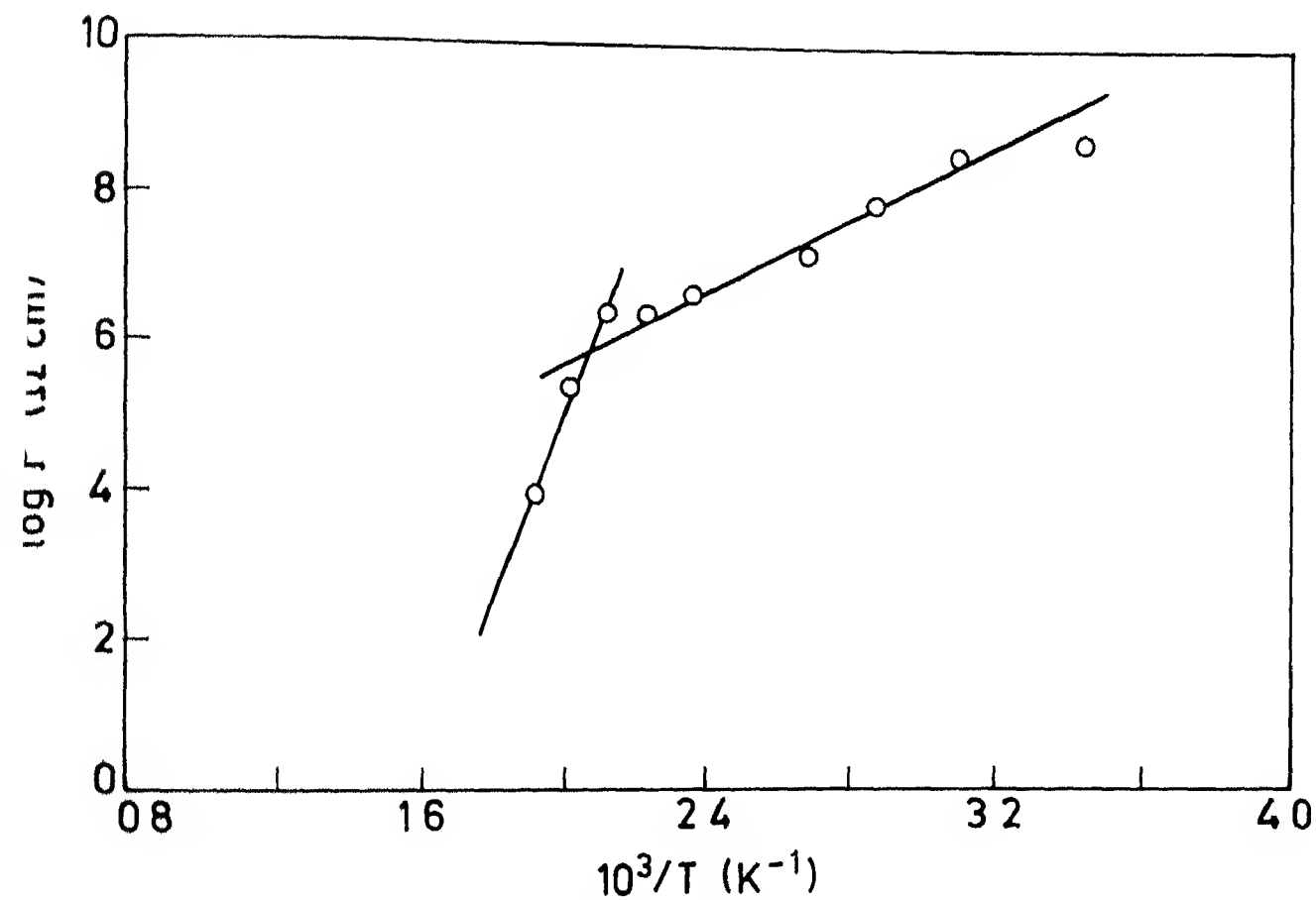


Fig 3 18 20 $\log P$ versus $1/T$ plot for glass sample A2

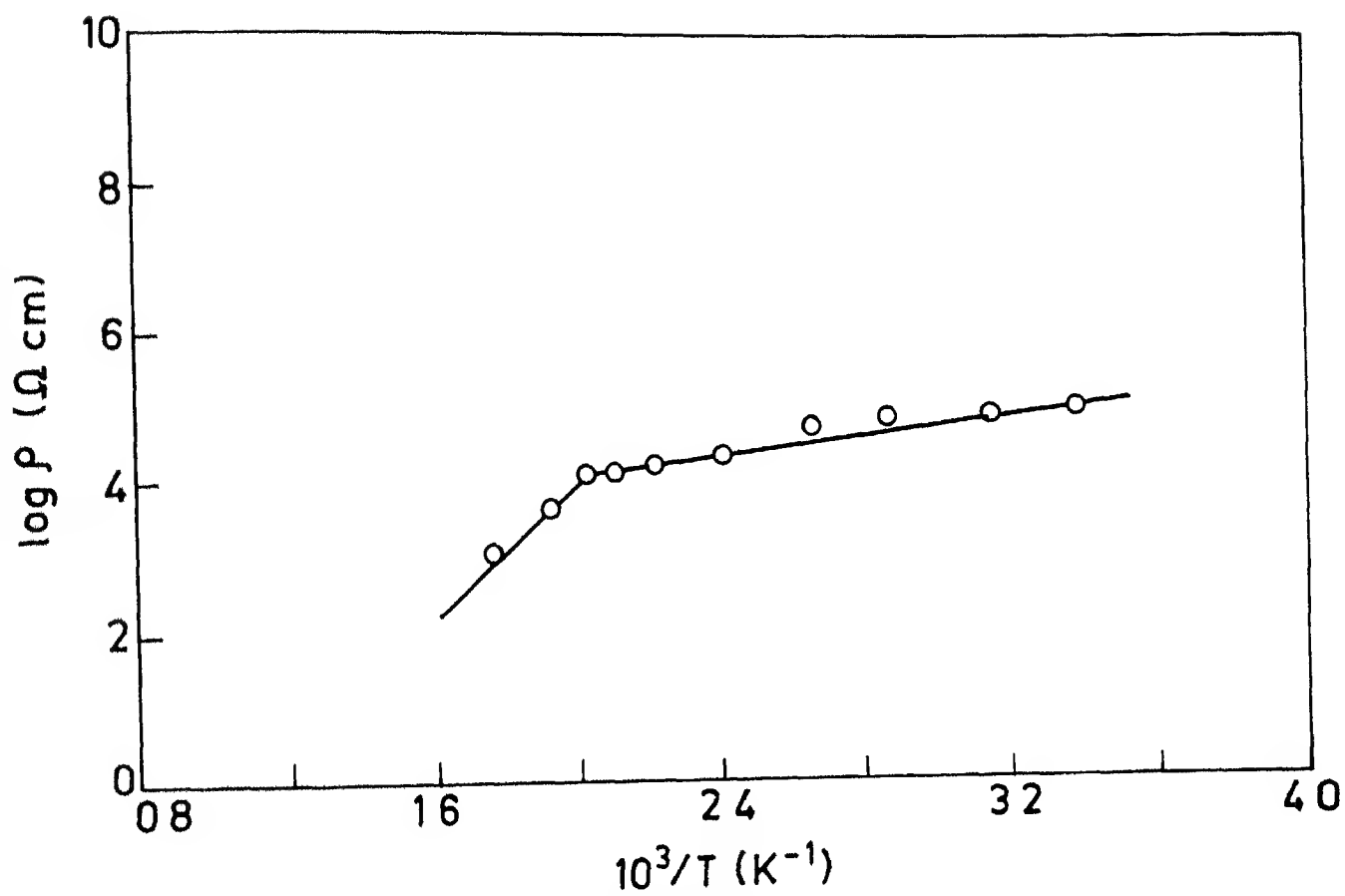


Fig 3 19 21 $\log \rho$ versus $1/T$ plot for glass sample A3

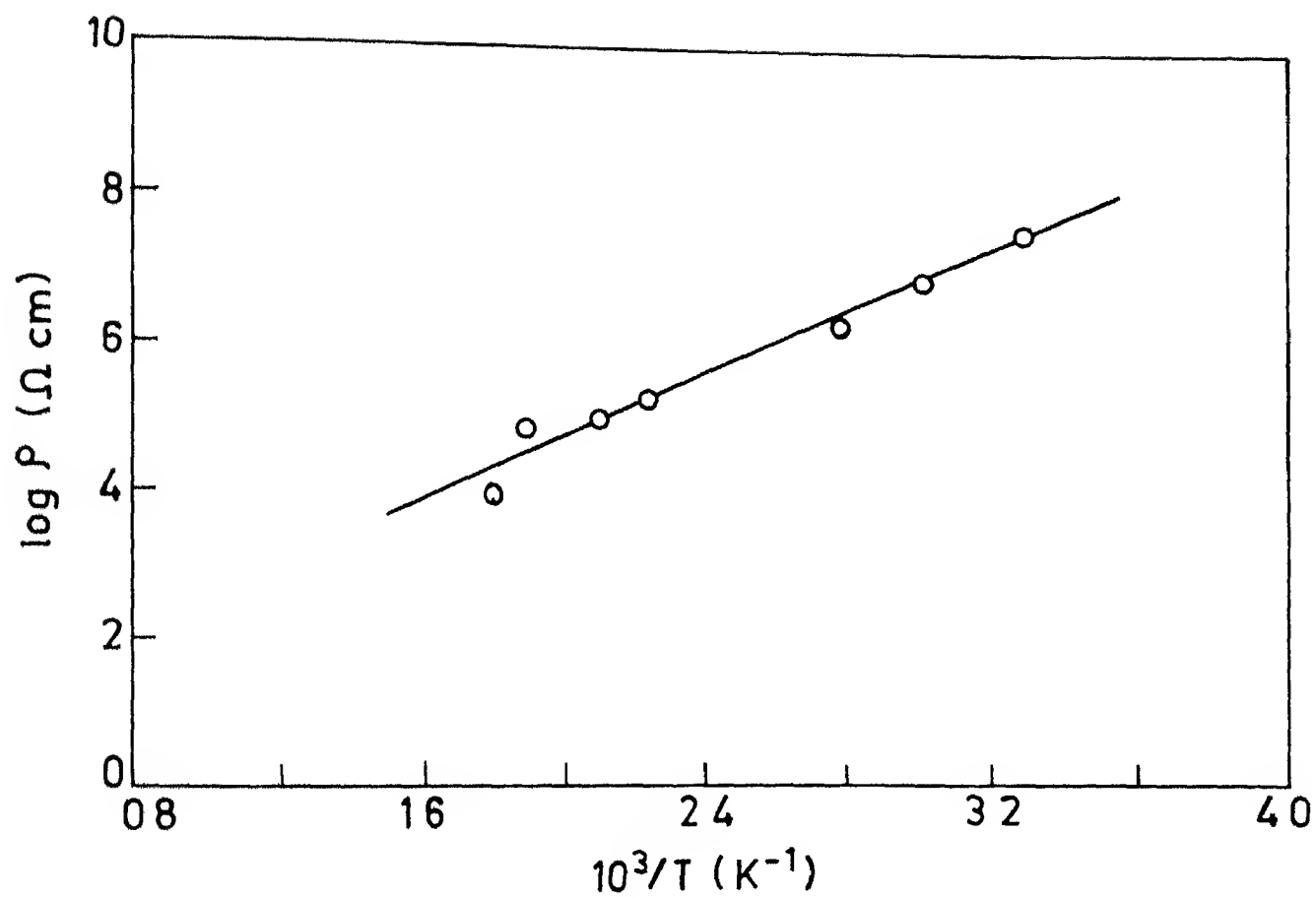


Fig 3 20 22 $\log P$ versus $1/T$ plot for glass sample A4

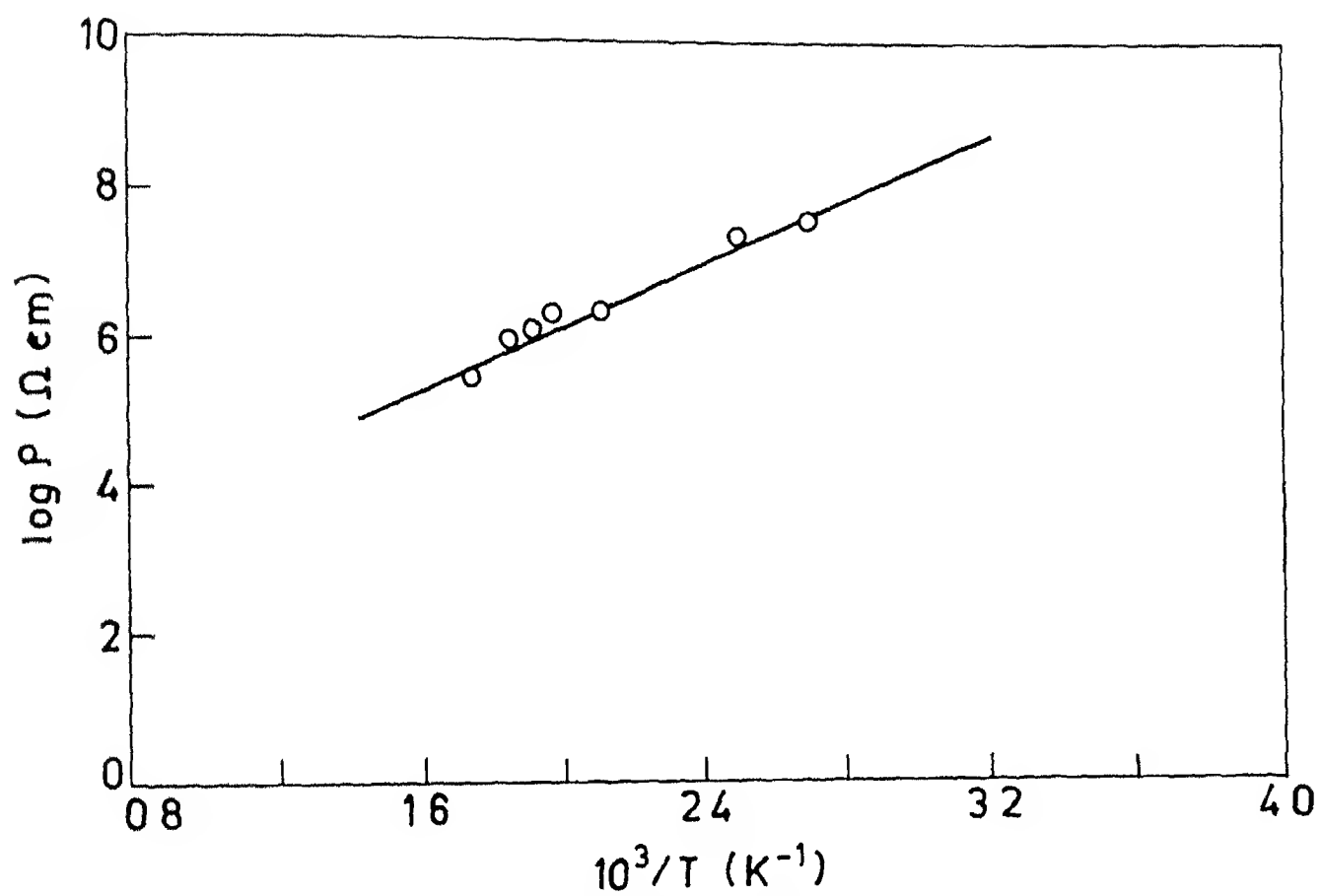


Fig 3 21 23 $\log P$ versus $1/T$ plot for glass sample IA1

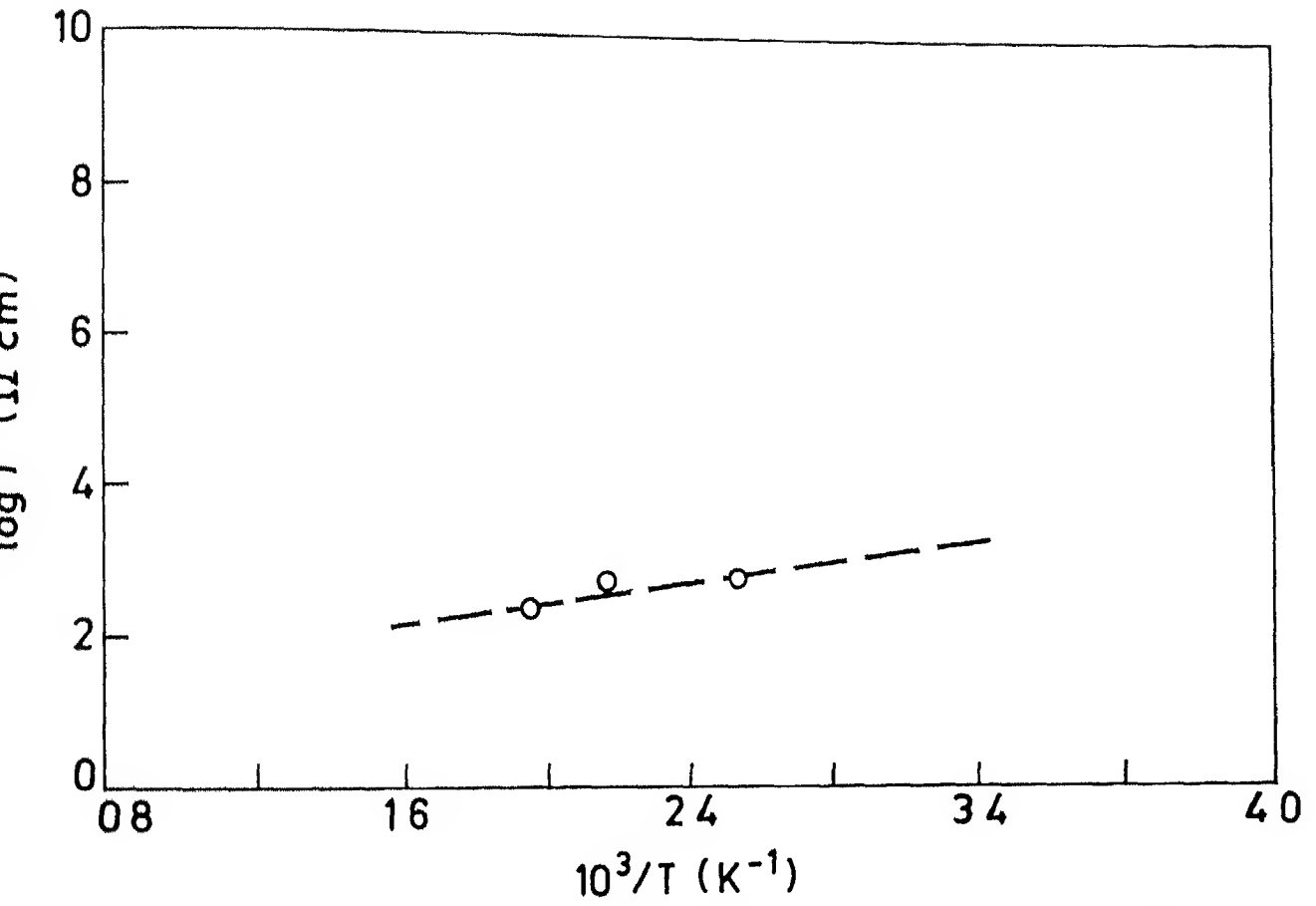


Fig 3 22 24 $\log P$ versus $1/T$ plot for glass sample IA 2

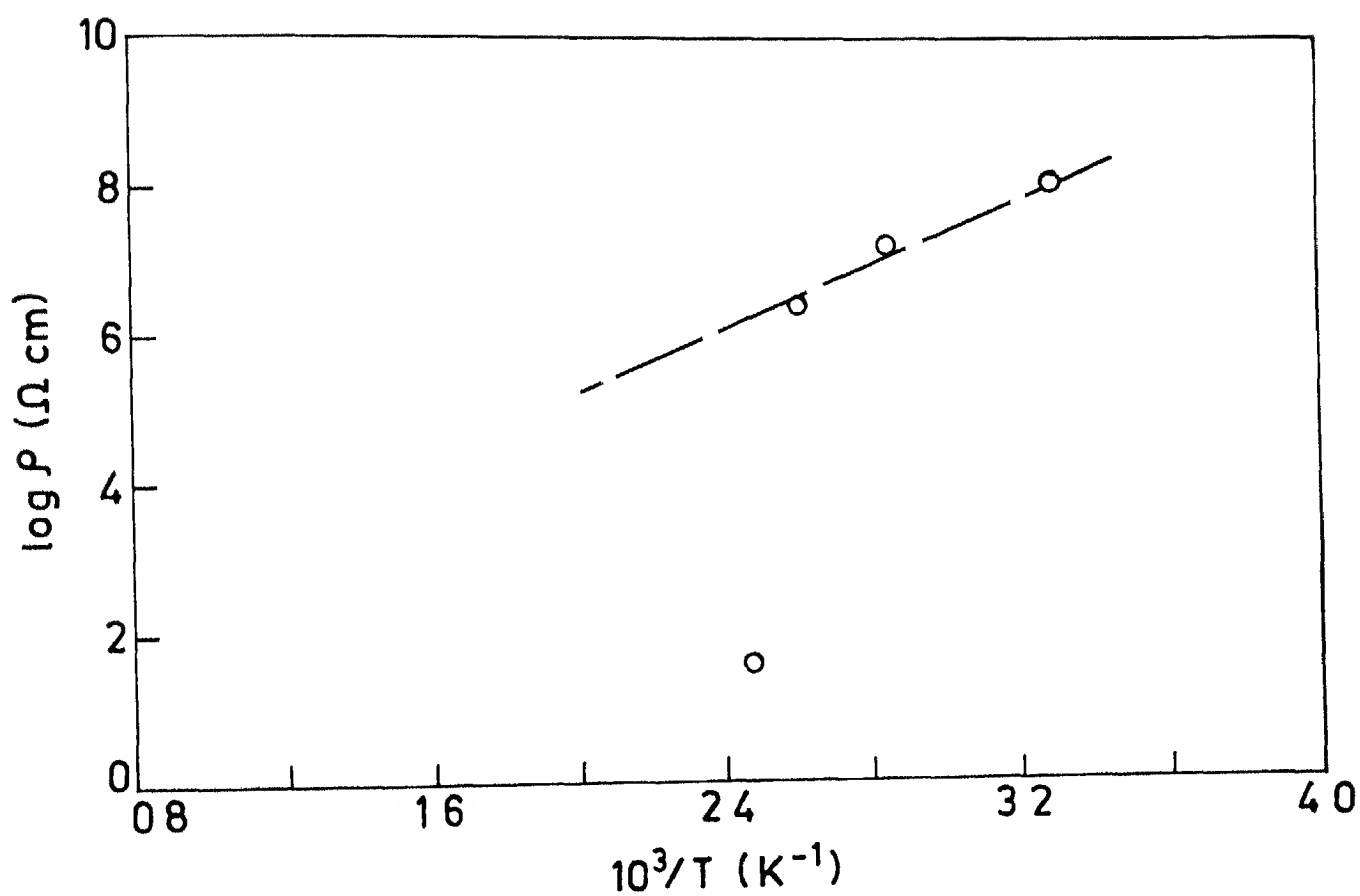


Fig 3 23 25 $\log \rho$ versus $1/T$ plot for glass sample IA3

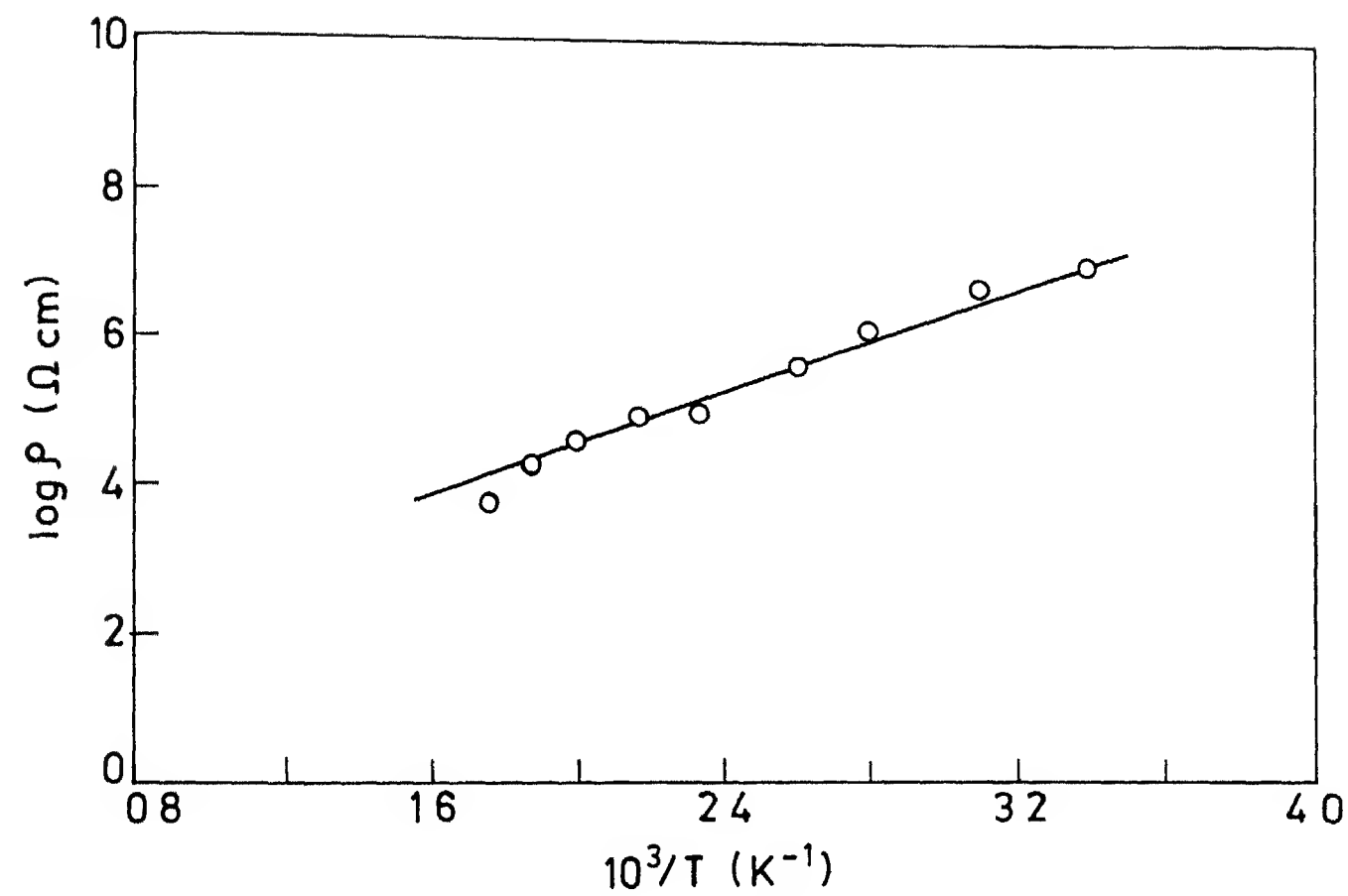


Fig 3 24 26 $\log \rho$ versus $1/T$ plot for glass sample IA4

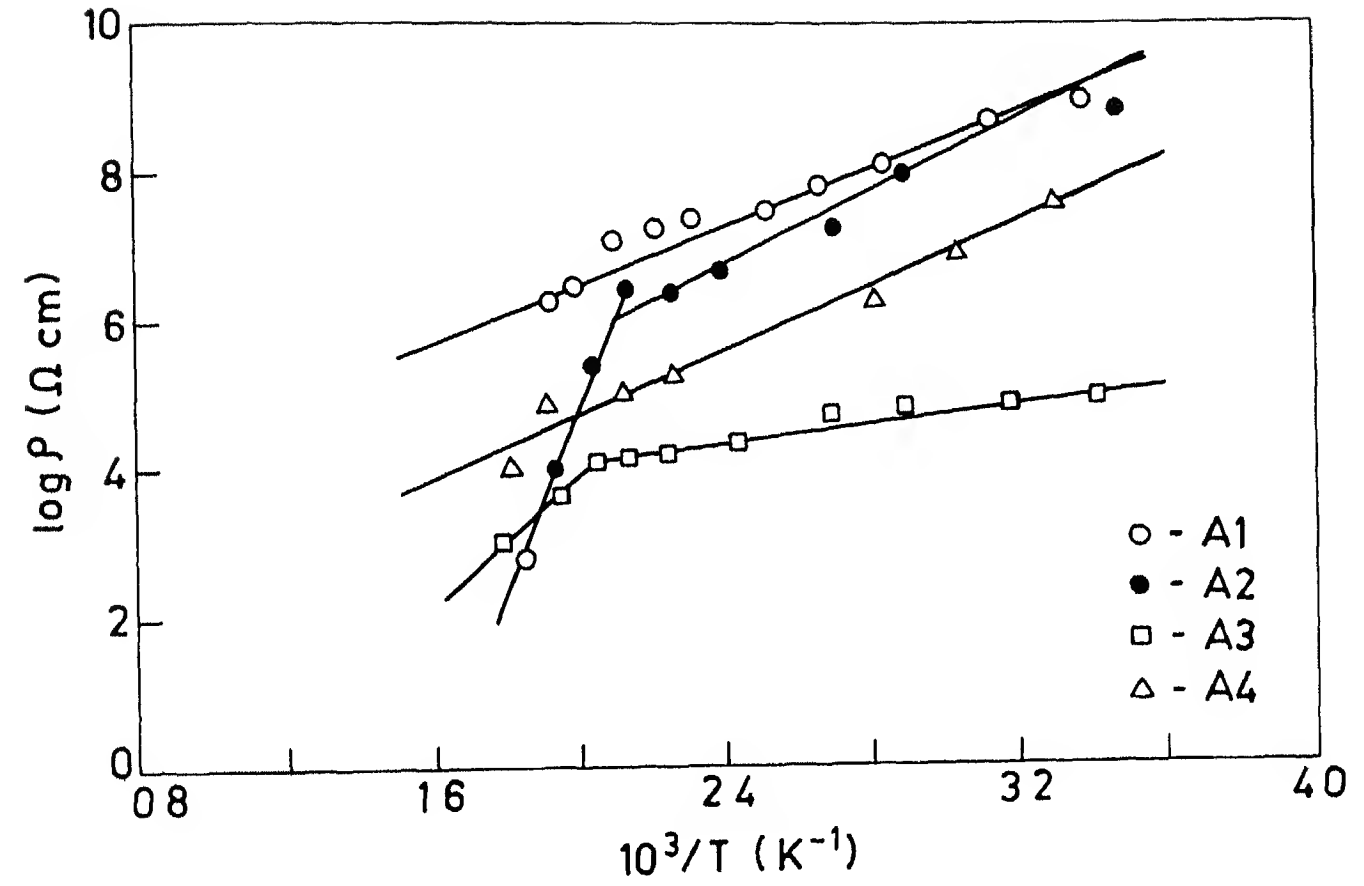


Fig 3 25 27 $\log P$ versus $1/T$ plot for glasses A1, A2, A3, A4

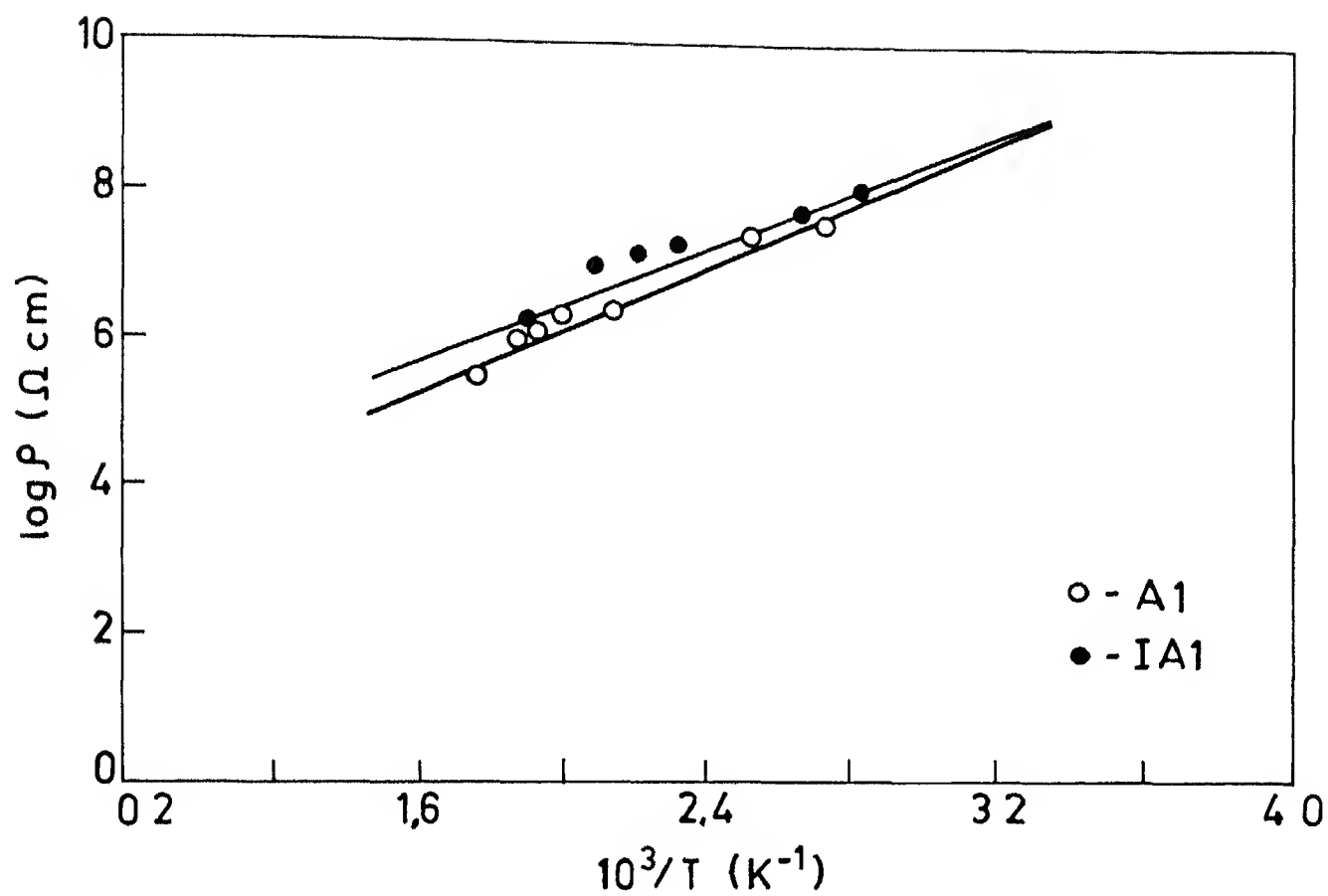


Fig 3 26 28 $\log \rho$ versus $1/T$ plot for glass samples A1 and IA1

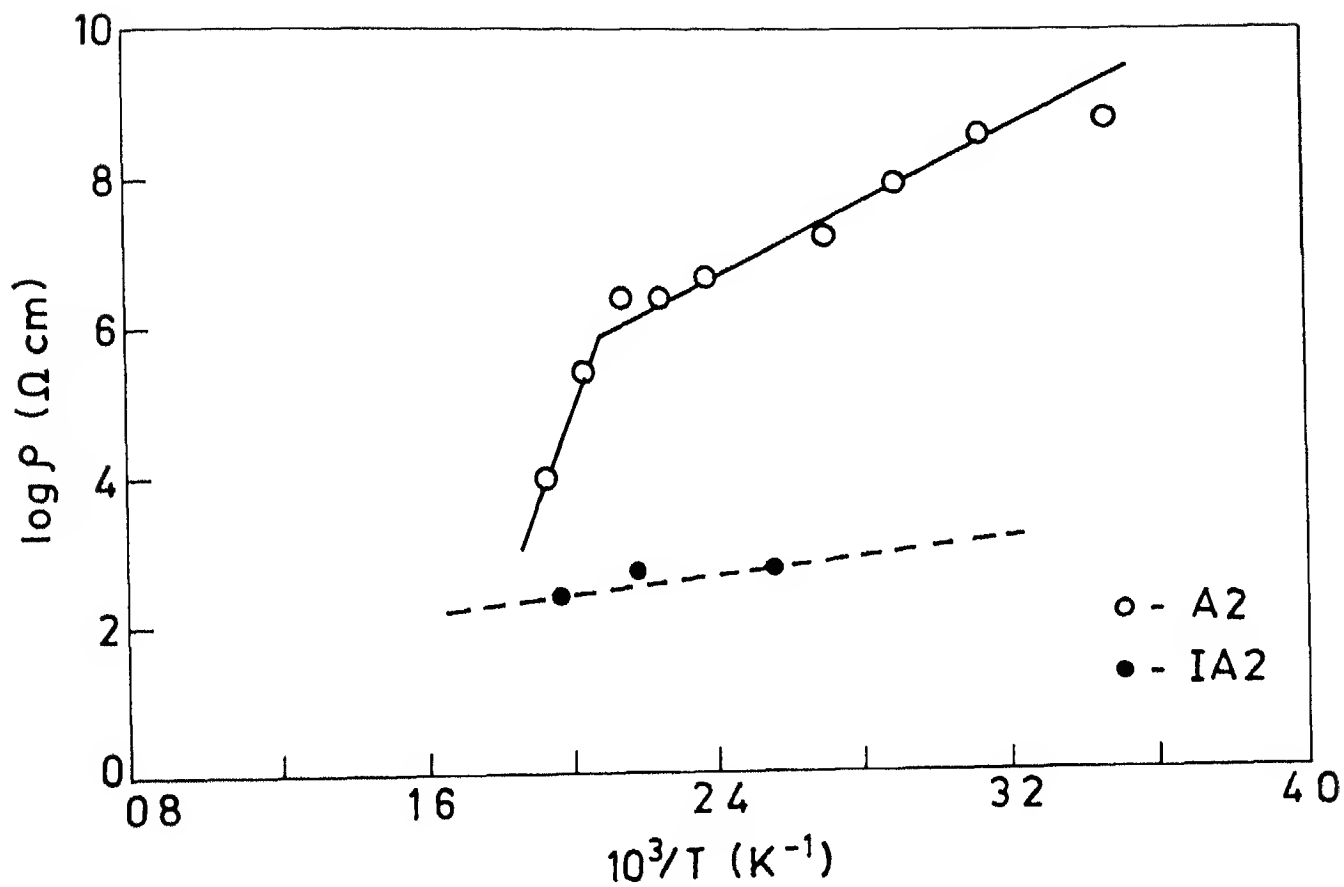


Fig 3 27 29 $\log \rho$ versus $1/T$ plots for glass samples A2 and IA2

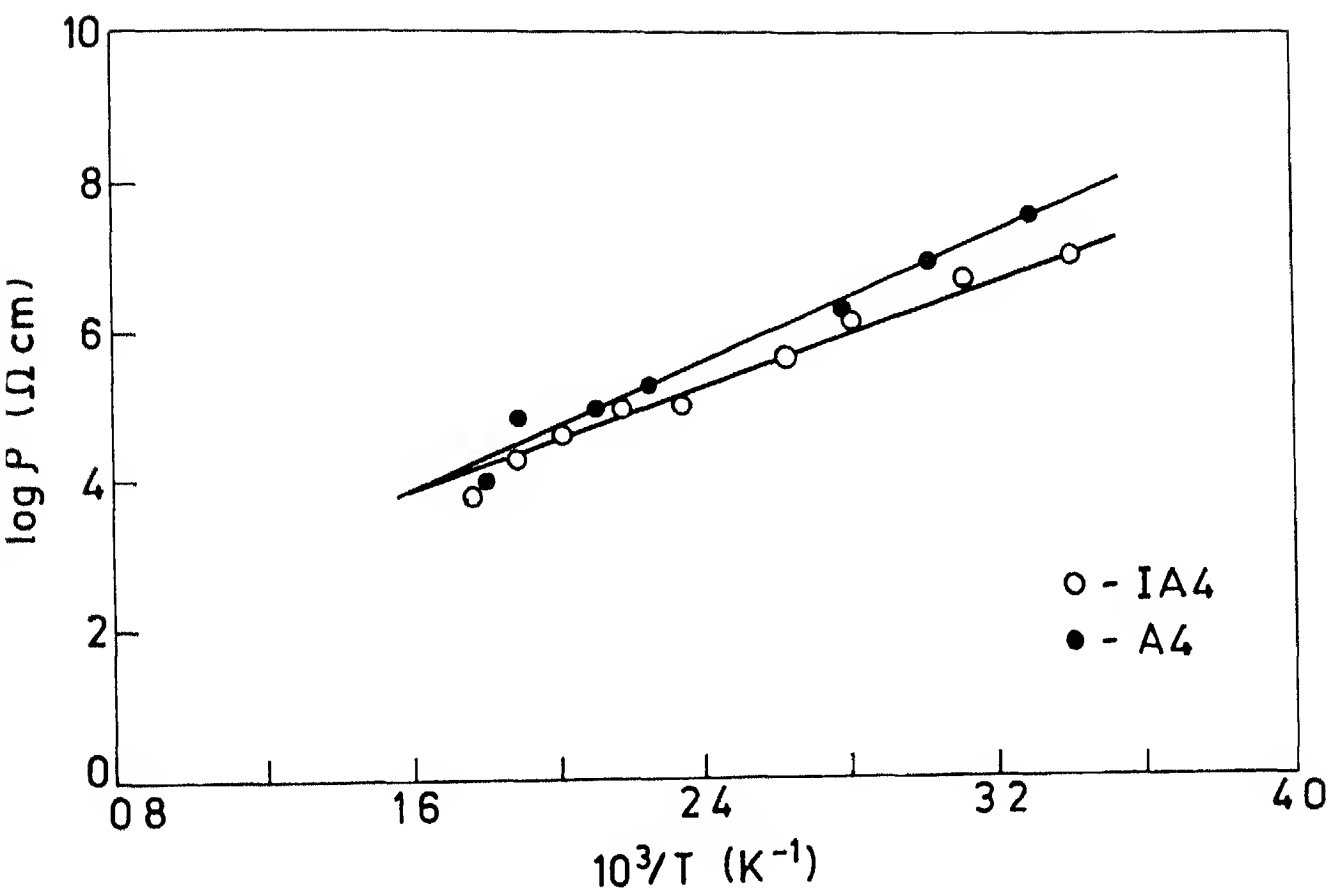


Fig 3 28 30 $\log \rho$ versus $1/T$ plots for glass samples A4 and IA4

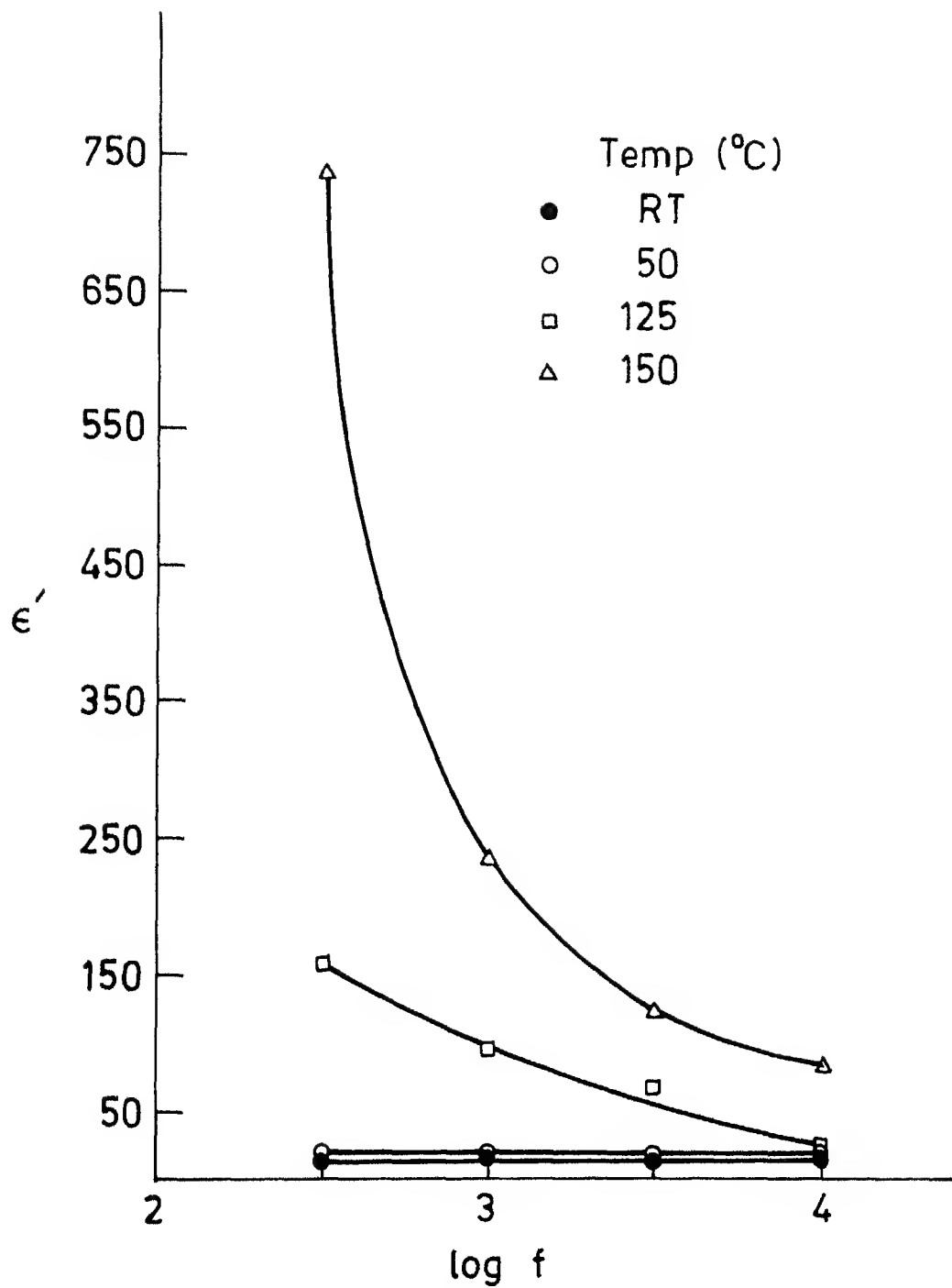


Fig 3 29 31 ϵ' versus $\log f$ Plot for Glass Sample A1

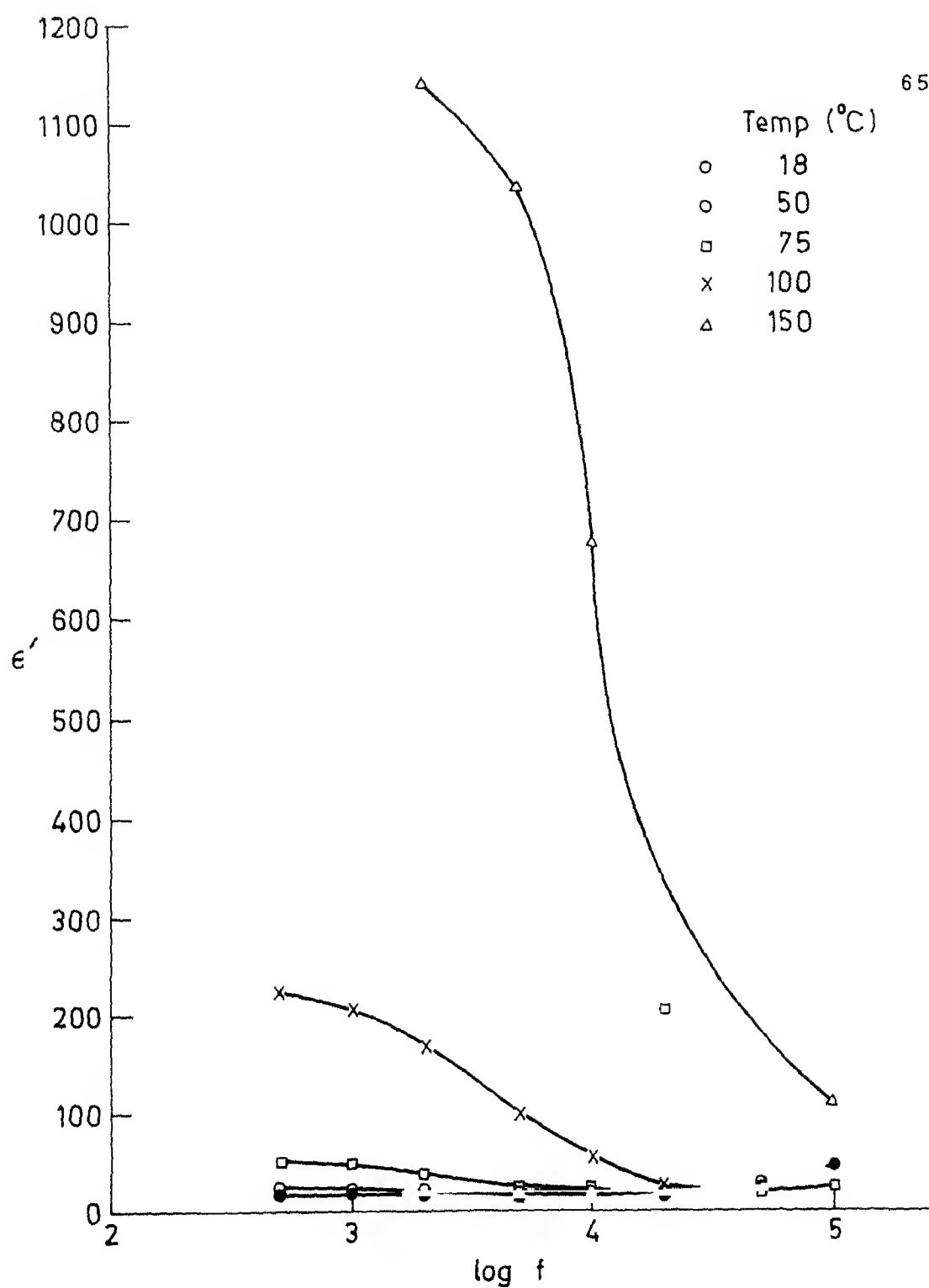


Fig 33032 ϵ' versus log f Plot for Glass Sample A2

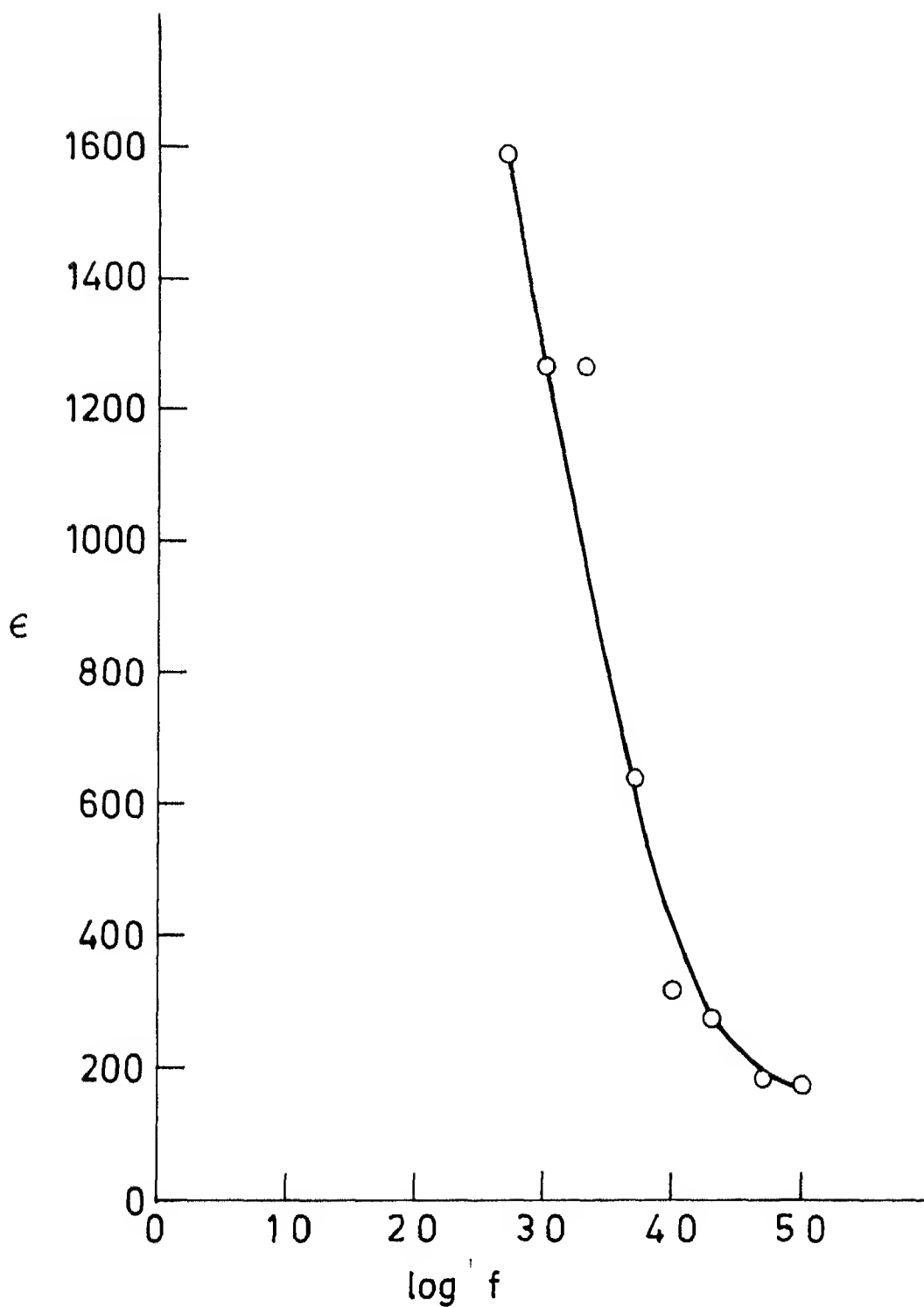


Fig 3 31 33 ϵ' versus $\log f$ Plot for Glass Sample A3 ($T = 103^\circ\text{C}$)

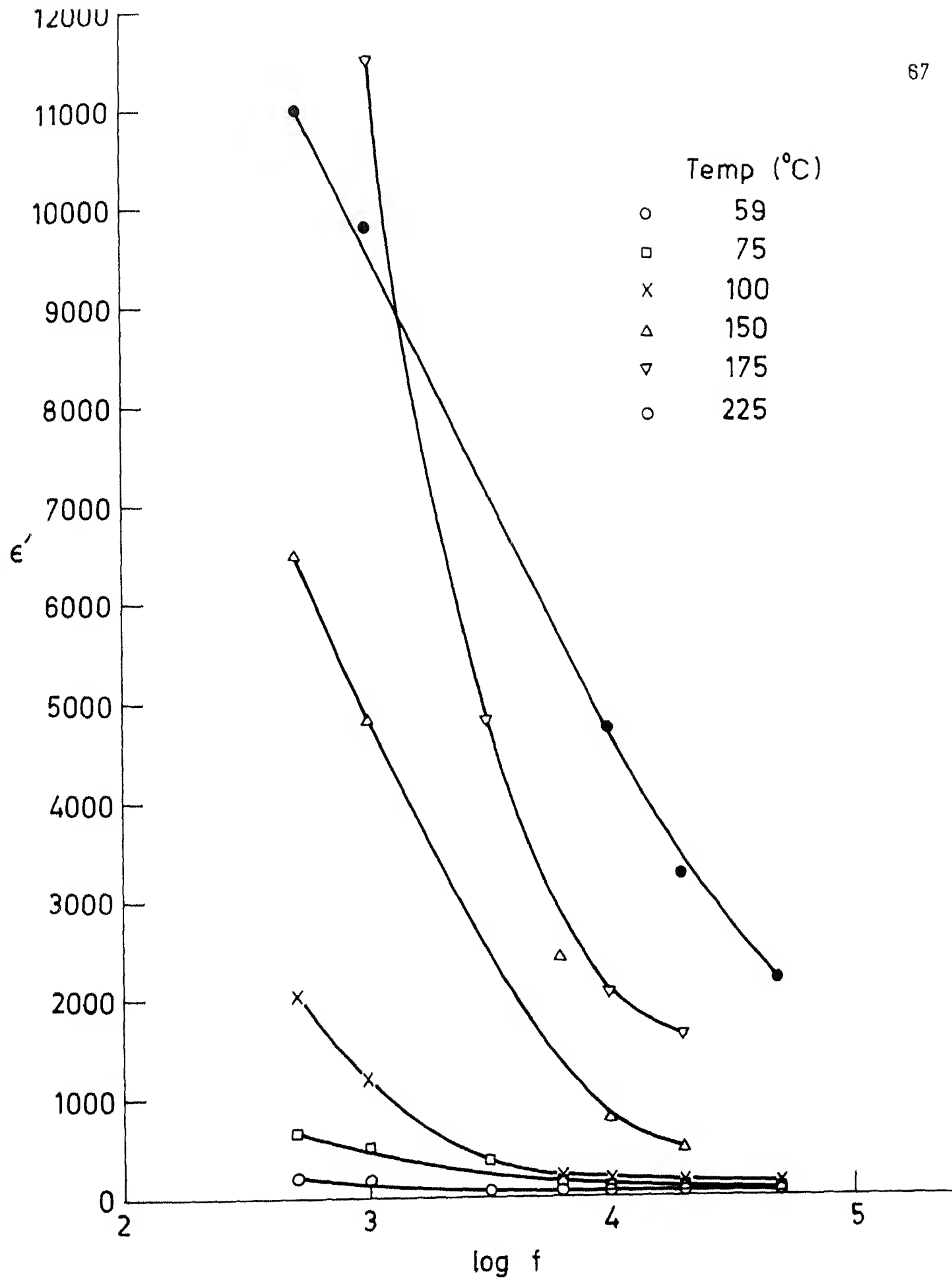


Fig 3 32 34 ϵ' versus log f Plot for Glass Sample A4

REFERENCES

- 1 C R Bamford, Colour Generation and Control in Glass, Glass Science and Technology 2, (Elsevier Scientific Pub. Co 1977)
- 2 D Chakravorty, Preparation and Characterization of Materials, ed , C N R Rao and J M Honing (Academic Press, London, in Press)
- 3 S.D Stooky, U.S Patent No 2515275, 1950
- 4 S D Stooky, Byt Patent No 752243, 1956
- 5 Roger J Araujo, Treatise on Materials Science and Technology, Vol 12 (Academic Press, London, 1977) P 91
- 6 T P Seward III, J Non-Cryst Solids 40 (1980), 499
7. G A Niklasson and C G Granqvist, J Appl Phys 50 (8), 5500 (1979)
- 8 H Rawson, Props and Applications of Glasses, Glass Science and Technology, 3, p 218.
- 9 Ashok Shrivastava, Ph D Thesis, I I T Kanpur
10. D. Chakravorty, A R Haranahalli and D Kumar, Phys Stat Solidi (a), 51 (1975) 275.
- 11 D Chakravorty, Appl Phys Lett , 24 (2) (1974) 62
12. Ashok Shrivastawa, Ph D Thesis, I I T Kanpur.
13. W.A Weyl, Coloured Glasses, Society of Glass Tecmology, 1951.
14. P W McMillan, Glass Ceramics, 2nd Edition (Academic Press, London, 1979)
15. H Rawson, Phys Chem Glasses 6 (1965) 81.

- 16 D Chakravorty, French Patent 31218 (1972)
- 17 D Chakravorty, A K Bandyopadhyay and V K Nagesh, J
Phy D Appl Phys Vol 10 (1977), 2077
- 18 R H Doremus, J Chemical Phys 40 (1964) 2389
- 19 R H Doremus, J Chemical Phys 42 (1965) 414
- 20 D Chakravorty, J Non-Crystalline Solids 15 (1974) 191
21. G C Das, Ph.D Thesis, I I T Kanpur
- 22 S Chakravorty, M Tech Thesis, I I T Kanpur
- 23 R H Doremus, A M Turkalo, J Mater Sc 11 (1976) 903
- 24 D Chakravorty, A Shuttleworth, P H Gaskell, J Mater
Science, 10 (1975) 799
- 25 P Sarkar, D Chakravorty and J Kumar, J Mater Science,
18 (1983) 250
- 26 M A Smithhard, Solid State Comm 13 (1973) 153
27. M A Smithhard and R Dupree, Phys Status Solidi
A11 (1972) 695
- 28 D Chakravorty and C S Murthy, 1975, J Phys D
Appl Phys 8 L162
- 29 C.A Neugebauer and M B Webb, J Appl Phys
33 (1962) 74
30. W.H Omar, M E I Hamamsy and A Bishay, Proc 9th
Int Congr on Glass Versailles (1971) 521.
- 31 D. Eaton, J. Am Ceramic Soc 47 (1964) 554
32. H Jain, J of Non-Crystalline Solids 66 (1984) 157
- 33 R. Syed, Ph D Thesis, Catholic University of America,
Washington, D.C (1983)

1

98043

MSP-1986-M-SIN-ELE